



Original article

Metabolic stability optimization and metabolite identification of 2,5-thiophene amide 17 β -hydroxysteroid dehydrogenase type 2 inhibitors

Emanuele M. Gargano^a, Enrico Perspicace^a, Nina Hanke^c, Angelo Carotti^d,
Sandrine Marchais-Oberwinkler^{a, **}, Rolf W. Hartmann^{a, b, *}

^a Pharmaceutical and Medicinal Chemistry, Saarland University, Campus C2₃, D-66123 Saarbrücken, Germany

^b Helmholtz Institute for Pharmaceutical Research Saarland (HIPS), Campus C2₃, D-66123 Saarbrücken, Germany

^c ElexoPharm GmbH, Campus A1₂, D-66123 Saarbrücken, Germany

^d Dipartimento Farmaco-Chimico, Università degli Studi di Bari, V. Orabona 4, I-70125 Bari, Italy

ARTICLE INFO

Article history:

Received 23 July 2014

Received in revised form

16 September 2014

Accepted 18 September 2014

Available online 20 September 2014

Keywords:

17 β -HSD2

Osteoporosis

Metabolic stability

Metabolite identification

cLogP

Inhibitor design

ABSTRACT

17 β -HSD2 is a promising new target for the treatment of osteoporosis. In this paper, a rational strategy to overcome the metabolic liability in the 2,5-thiophene amide class of 17 β -HSD2 inhibitors is described, and the biological activity of the new inhibitors. Applying different strategies, as lowering the cLogP or modifying the structures of the molecules, compounds **27**, **31** and **35** with strongly improved metabolic stability were obtained. For understanding biotransformation in the 2,5-thiophene amide class the main metabolic pathways of three properly selected compounds were elucidated.

© 2014 Elsevier Masson SAS. All rights reserved.

1. Introduction

Osteoporosis [1] is a systemic disease in which an unmatched activity of osteoclasts and osteoblasts leads to a decline in bone density and quality. It is also correlated with an increased risk of bone fracture. Osteoporosis is observed in 40% of postmenopausal women [2]. Considering the progressive aging of the population this number is expected to constantly increase in the near future [3] and osteoporosis is therefore considered as a serious public health concern.

The available therapies today (bisphosphonates and selective estrogen receptor modulators) lack of a satisfying profile in terms of safety and efficacy. Bisphosphonates, with alendronate as the principal drug used in the treatment of osteoporosis, are effective in both postmenopausal women [4] and men [5,6], though they are able to reduce the risk of fracture by only 50% and are associated with side effects such as osteonecrosis of the jaw. Raloxifene is, among the selective estrogen receptor modulators (SERMs), one of the most often used compounds for the treatment of osteoporosis [7]. SERMs are efficient too, but, as bisphosphonates, endowed with several side effects, such as an increased risk of venous thromboembolism. As a consequence, the finding of new, safer and more effective treatments for osteoporosis is of particular importance for public health.

It has been proven that an important player in the maintenance of bone health is the physiological, pre-menopausal concentration of the estrogen estradiol (E2). That induces bone formation and represses bone resorption by acting on the osteoblasts [8]. Estrogen replacement therapy (ERT) was used in the past in postmenopausal osteoporosis patients [9,10], successfully reducing the risk of fractures but increasing the incidence of cardiovascular diseases and breast cancer [10,11], which was the reason for the cessation of this

Abbreviations: 17 β -HSD2, 17 β -hydroxysteroid dehydrogenase type 2; 17 β -HSD1, 17 β -hydroxysteroid dehydrogenase type 1; E1, estrone; E2, 17 β -estradiol; T, testosterone; DHT, dihydrotestosterone; DHEA, dehydroepiandrosterone; A-dione, Δ 4-androstene-3,17-dione; FC, flash chromatography; s.f., selectivity factor; RBA, relative binding affinity; ER, estrogen receptor; ERT, estrogen replacement therapy; inh, inhibition; MEP, molecular electrostatic potential; UDPGA, uridine diphosphate glucuronic acid; PAPS, 3'-phosphoadenosine-5'-phosphosulfate.

* Corresponding author. Pharmaceutical and Medicinal Chemistry, Saarland University, Campus C2₃, D-66123 Saarbrücken, Germany.

** Corresponding author.

E-mail addresses: s.marchais@mx.uni-saarland.de (S. Marchais-Oberwinkler), rw@mx.uni-saarland.de, rolf.hartmann@helmholtz-hzi.de (R.W. Hartmann).

therapy. It has also been shown that testosterone (T) has beneficial effects on bone formation [12,13].

Hence, an optimal strategy for the treatment of osteoporosis should be that to inducing a local increase in E2 concentration in bone tissue, without affecting the systemic levels of E2. Such an effect might be achieved by inhibiting 17 β -hydroxysteroid dehydrogenase type 2 [14] (17 β -HSD2), an enzyme that catalyzes the conversion of the highly active 17 β -hydroxysteroids into the low inactive 17-ketosteroids, that is the estrogen E2, and the androgen testosterone (T) into their inactive oxidated forms estrone (E1) and Δ^4 -androstene-3,17-dione (A-dione), respectively (Chart 1). The biological counterparts, 17 β -hydroxysteroid dehydrogenase type 1 (17 β -HSD1) and 17 β -hydroxysteroid dehydrogenase type 3 (17 β -HSD3) catalyze the reverse reactions. Inhibitors of 17 β -HSD1 are potential drugs for the treatment of breast cancer and endometriosis and have recently been described in a series of papers by us [15–18].

As 17 β -HSD2 is expressed in osteoblastic cells [19–21], its inhibition should lead to the desired local increase of E2 and T levels in bone tissue.

Ideally, the new 17 β -HSD2 inhibitors should, in addition to their activity on the target enzyme, be selective over 17 β -HSD1 and should have no affinity for the estrogen receptors (ER) α and β in order to avoid E2 related side effects.

The discovery of potent and selective nonsteroidal inhibitors of 17 β -HSD2 has been already reported by our research group [22–30].

As drugs encounter formidable challenges to their stability in vivo, it is not sufficient to only focus on potency in the development process of a drug candidate. It is also important to profile the metabolic stability of a lead series and improve it when this constitutes a potential liability. As 17 β -HSD2 should be inhibited with constancy to locally increase the E2 levels and to maintain them high over the time needed to re-establish bone metabolism, the development of very metabolically stable inhibitors is particularly important. The enhancement of the metabolic stability of a class of inhibitors is a very difficult task for the medicinal chemist but could strongly favor the emergence of potential preclinical candidates [31].

As a consequence, we decided to test three of our most promising, previously reported 17 β -HSD2 inhibitors (compounds 1–3) for their metabolic stability in human liver microsomes S9 fraction (Chart 2), a powerful tool to explore both phase I and phase II major metabolic reactions [32]. 1, 2 and 3 represent very good compounds in terms of enzymatic inhibitory potency and selectivity over 17 β -HSD1, however, they do not exhibit a satisfying stability displaying short half-lives between 4 and 38 min.

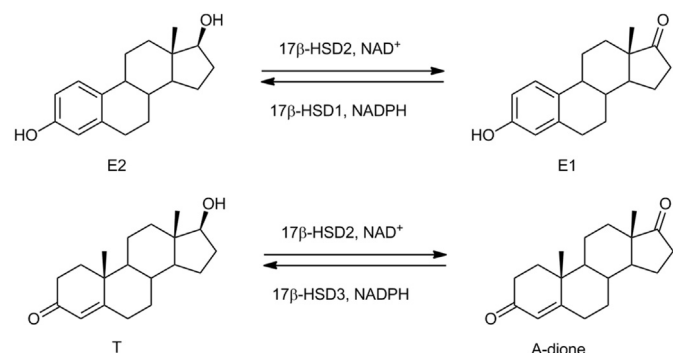


Chart 1. Interconversion of estradiol (E2) to estrone (E1) by 17 β -HSD2 and 17 β -HSD1, and testosterone (T) to androstenedione (A-dione) by 17 β -HSD2 and 17 β -HSD3.

In this report, we describe the analysis of the metabolic profile of some representative in house inhibitors, the design of new, more stable inhibitors based on the results from these studies, as well as their synthesis and biological evaluation. In addition three inhibitors were investigated for their specific metabolic fate in order to understand the particular biotransformation of this class of molecules.

2. Inhibitor design

2.1. Stability towards human S9 fraction

Different hepatic enzymes can be responsible for the metabolic transformation of a compound and it frequently happens that small structural changes on the molecule lead to a switch of the responsible metabolic enzyme [33], a phenomenon known as “metabolic switching” [33]. As a consequence introduction of several structural changes in the scaffold of a compound is not an appropriate method to evaluate liabilities of single moieties as changes in the core structure could have switched the main site of metabolism.

Therefore a set of 11 selected compounds described by our group [24,25] and carefully chosen as differing from one another by one structural change only, were tested for their phase I and II metabolic stability using human liver S9 fraction (Table 1), in order to find out the potential sites of metabolism.

From the comparison of compound 1 with 2 ($t_{1/2}$ = 17 min and 38 min, respectively) it appears that the methoxy group on the A ring in *meta* position is unfavorable for metabolic stability compared to the methyl group, whereas the presence of a *meta* dimethyl amino group (compound 4, $t_{1/2}$ = 29 min) provides a similar stability as the methylated derivative 2 ($t_{1/2}$ = 38 min).

The exchange of the methoxy group (5) for a methyl (6) on the C ring results also in a slight increase in metabolic stability ($t_{1/2}$ = 12 min for 5 vs. 20 min for 6).

Compound 5 bears an additional fluorine in *ortho* position on the A ring in comparison to compound 1. However introduction of this fluorine atom does not improve the stability of compound 5 (5, $t_{1/2}$ = 12 min vs. 17 min for 1).

Comparison of the unsubstituted inhibitor 7 ($t_{1/2}$ = 38 min), with 8 ($t_{1/2}$ = 1 min) bearing a hydroxy group on the A ring and with 9 ($t_{1/2}$ = 4 min) having an OH on the C ring shows that the phenolic OH group enhances the metabolic degradation of this class of compounds. This result was also observed in presence of a methylene linker in compound 3, bearing an OH on the C ring and having a half-life of 4 min. On the other hand, the nature of substituents on the A ring (in the presence of the OH group on the C ring) plays an important role in the stabilization, as addition of the methyl group alone (10, $t_{1/2}$ = 17 min) or a hydroxy group (11, $t_{1/2}$ = 20 min) slightly increases the metabolic stability. Compounds 3, 10 and 11, in comparison with compound 1 have in their core two additional potential metabolic sites: the methylene linker and the phenolic group (liable for phase II metabolic attack). Despite the increase in liable metabolic sites their half-lives ($t_{1/2}$ = 17 min and 21 min, respectively) are still in the range of compound 1.

In summary none of the tested inhibitors showed a satisfying metabolic stability profile (Table 1). However, from these results it is obvious that 1. The methyl group on the A ring is less prone to metabolic degradation than the methoxy group (compounds 1 and 2). 2. The phenolic hydroxy substituent on both the A ring or the C ring is subject to fast metabolism (compounds 8 and 9), which can be slightly slowed down by introduction of substituents on the other ring (compounds 10 and 11).

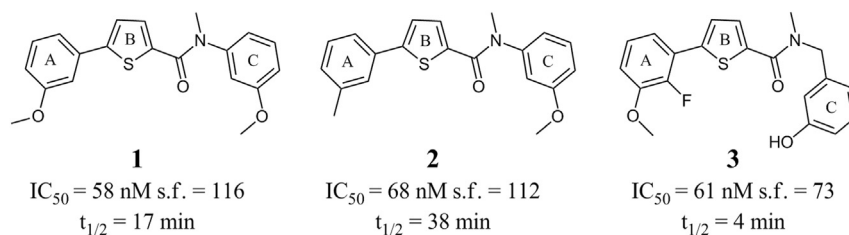


Chart 2. Previously described 17 β -HSD2 inhibitors.

2.2. Design of inhibitors

In the inhibitor design we took into account the information we had gained from the metabolic stability results. In addition we tried to modify some other moieties that have the potential of being metabolically labile. Doing this we kept in mind the structure-activity and structure-selectivity relationships obtained in our previous studies [24,25].

As the methyl group resulted to be more stable than the methoxy group on the A and C ring, we decided to exchange each methoxy group with a methyl function and then to explore the effect of this substitution pattern on both activity and metabolic stability. It was also observed that most of the compounds with a hydroxy group in the presence of the methylene linker, known to be a critical point for metabolism, scored the worst results in terms of metabolic stability. However since a hydroxy group is needed for activity [25] in the series of compounds having the methylene linker, we decided to stop further structural modifications on this series. Therefore compounds without linker with the general structure **A**, depicted in Chart 3 were synthesized.

The thiophene is also described as a potential site of metabolism [34]. Therefore, we tried to modify it by bioisosteric replacements using benzene, furane and thiazole (general structure **B**).

Moreover, it has been reported [35] that the lipophilicity parameters like cLogP can play an important role for the metabolic stability. Very often the simple strategy to lower the cLogP was appropriate to improve the metabolic stability of a compound. Therefore some inhibitors, modified at the A ring with a moiety reducing cLogP were designed (general structure **C**, Chart 3).

Furthermore, we profiled the metabolic pathway of the newly synthesized dimethylphenyl thiophene **12** (Chart 4) looking for the major metabolites resulting from the mono-oxidation of the phenylthiophene part (Chart 4).

In order to identify the main metabolites, especially the one coming from mono-oxidation of the phenylthiophene fragment, we synthesized different hydroxylated derivatives of **12** bearing one additional oxygen in the positions that are likely to be attacked by the metabolizing enzyme (represented by the general structures **D** and **E**, Chart 4).

3. Results

3.1. Chemistry

The synthesis of the 2,5-thiophene derivatives (compounds **12–23**, **25–27**, **36–38** and **40**) and the 2,5-furane derivatives (compounds **31–34**) is depicted in Scheme 1. The 5-bromothiophene-2-carboxylic acid chloride and the 5-bromofuran-2-carboxylic acid chloride were obtained from the corresponding carboxylic acids **36c** or **31b** by reaction with SOCl_2 and subsequently reacted with different anilines (Method A), providing the intermediates **12a–23a**, **25a–27a**, **36b**, **37b**, **40b** and **31a–34a** in good yields. Subsequently, Suzuki coupling (Method B) using

tetrakis(triphenylphosphine)palladium and cesium carbonate in a mixture DME/EtOH/H₂O (1:1:1, 3 mL) as solvent and microwave irradiation (150 °C, 150 W for 20 min), afforded the desired 2,5-thiophene derivatives **12–23**, **25–27**, **36a**, **37a**, **40a** and the 2,5-furane derivatives **31–34**. Methoxy compounds **36a** and **37a** were submitted to ether cleavage using boron trifluoride-dimethyl sulfide complex yielding the hydroxy compounds **36** and **37**. The aldehyde function of compound **40a** was reduced to primary alcohol using NaBH_4 to provide compound **40**. The synthesis of the 4-hydroxy-thiophene (compound **38**) is also depicted in Scheme 1 and followed the same synthetic pathway starting from the 5-bromo-4-methoxythiophene-2-carboxylic acid **38c**. The methoxy group in position 4 of the thiophene (compound **38a**) was cleaved using boron trifluoride-dimethyl sulfide complex and yielded the hydroxy compound **38**.

The synthesis of compound **30** was performed following the method depicted in Scheme 2. The intermediate **30b** was synthesized starting from 5-bromo-1,3-thiazole **30c** applying a Suzuki–Miyaura cross-coupling reaction with *m*-tolyl boronic acid, using microwave irradiation. The acidic hydrogen in position 2 of the thiazole **30b** was easily removed using *n*-butyl lithium. The anion obtained reacted immediately with a dry flow of carbon dioxide leading to the corresponding carboxylate **30a** which was subsequently activated using oxalyl chloride and reacted with 3-methyl-*N*-methylaniline to afford compound **30**.

The 1,4-disubstituted phenyl derivative **35** was obtained following a two-step procedure (Scheme 3). First, amidation was carried out by reaction of 4-bromobenzoyl chloride **35b** with *N*,3-dimethylaniline **35c** (Method A) providing the brominated intermediate **35a**. Suzuki coupling (Method B) afforded the final product **35**.

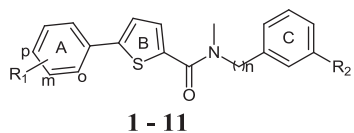
The synthesis of the 3-hydroxy-*N*-methyl-*N*,5-di-*m*-tolylthiophene-2-carboxamide (compound **39**) is depicted in Scheme 4. The ethyl 3-hydroxy-5-(*m*-tolyl)thiophene-2-carboxylate (compound **39d**) was obtained through the Fiesellmann thiophene synthesis [36] by reaction of the β -ketoester **39e** and the ethyl thioglycolate **39f**, according to the described procedure [36]. The hydroxy group of compound **39d** was protected using MeI to afford compound **39c** in a moderate yield. The saponification of the ester function of **39c** was carried out using potassium hydroxide in water/THF (1:1) mixture, affording the corresponding carboxylic acid **39b**. Amidation was performed by reaction of **39b** with *N*,3-dimethylaniline, using the standard condition (method A), leading to the methoxy compound **39a**. The methoxy group of **39a** was cleaved, using boron trifluoride-dimethyl sulfide complex and yielded the hydroxy derivative **39**.

3.2. Biological

3.2.1. Inhibition of human 17 β -HSD2 and selectivity over human 17 β -HSD1 in cell-free assays

The synthesized compounds were tested for their ability to inhibit 17 β -HSD2 and 17 β -HSD1 using enzymes from placental

Table 1
Half-life in human liver microsomes S9 fraction.



Compd.	R ₁	R ₂	n	Inhibitor t _{1/2} (min)
1	<i>m</i> -OMe	-OMe	0	17 ^a
2	<i>m</i> -Me	-OMe	0	38 ^a
3	<i>o</i> -F, <i>m</i> -OMe	-OH	1	4 ^{b,c}
4	<i>m</i> -N(Me) ₂	-OMe	0	29 ^a
5	<i>o</i> -F, <i>m</i> -OMe	-OMe	0	12 ^{b,c}
6	<i>o</i> -F, <i>m</i> -OMe	-Me	0	20 ^a
7	-H	-H	0	38 ^{b,c}
8	<i>m</i> -OH	-H	0	1 ^{b,c}
9	-H	-OH	0	4 ^{b,c}
10	<i>m</i> -Me	-OH	1	17 ^a
11	<i>o</i> -OH	-OH	1	21 ^a

^a Inhibitor tested at a final concentration of 3 μM, 1 mg/ml, pooled human liver S9 fraction (IVT, Xenotech or TCS Cellworks), 1 mM NADPH regenerating system, 0.75 mM UDPGA, 0.05 mM PAPS, incubated at 37 °C for 0, 5, 15, 30 and 45 min.

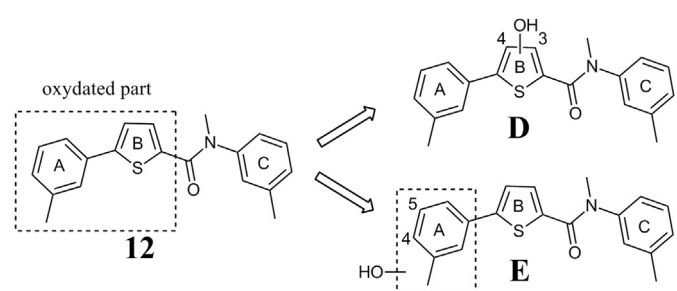
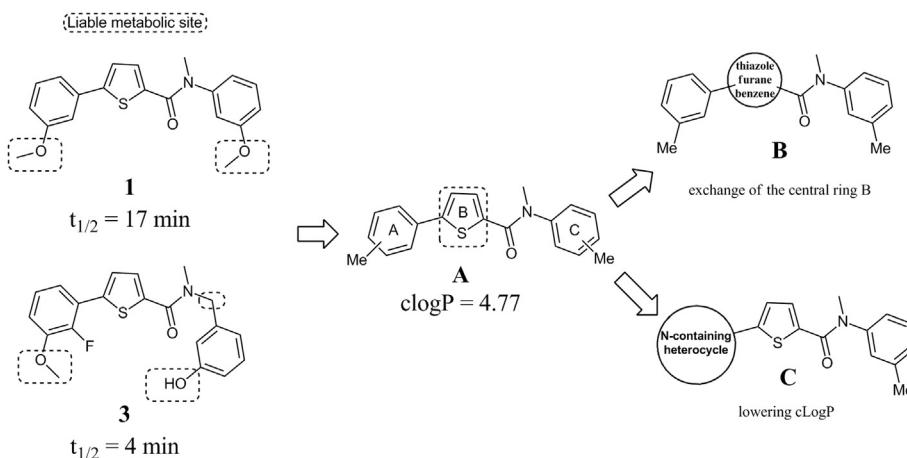
^b Inhibitor tested at a final concentration of 1 μM, 1 mg/ml pooled mammalian liver S9 fraction (BD Gentest), 2 mM NADPH regenerating system, 1 mM UDPGA and 0.1 mM PAPS, incubated at 37 °C for 0, 5, 15 and 60 min.

^c Mean of at least two determinations, standard deviation less than 25%.

3.2.1.1. Influence of lipophilic substituents on rings A and C. In the 2,5-thiophene class the methoxy groups in rings A and C can be replaced by methyl groups, without significantly affecting 17β-HSD2 inhibitory potency and selectivity over 17β-HSD1, as it becomes apparent from comparing **1**, **2** and **12** (IC₅₀ = 58 nM, s.f. = 116; 68 nM, s.f. = 112; 52 nM, s.f. = 83, respectively). This suggests that the methoxy groups on both rings do not function as H bond acceptors. Most likely the methyl substituents, being either part of a methoxy group or being directly connected to rings A and C, form important lipophilic interactions with the enzyme. This assumption is further supported by comparison of **12** with the corresponding compound without substituents on rings A and B, **24** [25], which is only moderately active (percent inhibition at 1 μM, 48%).

Encouraged by this result, nine compounds including all possible combinations of methyl substitutions on ring A and C were synthesized (compounds **12–20**), in order to investigate the influence of the methyl group position on the biological profile in this class of compounds. The substitution pattern indeed appears to be critical for both the 17β-HSD2 inhibitory potency and the selectivity over 17β-HSD1 as indicated by the wide range of inhibitory activities displayed by compounds **12–20** (Table 2).

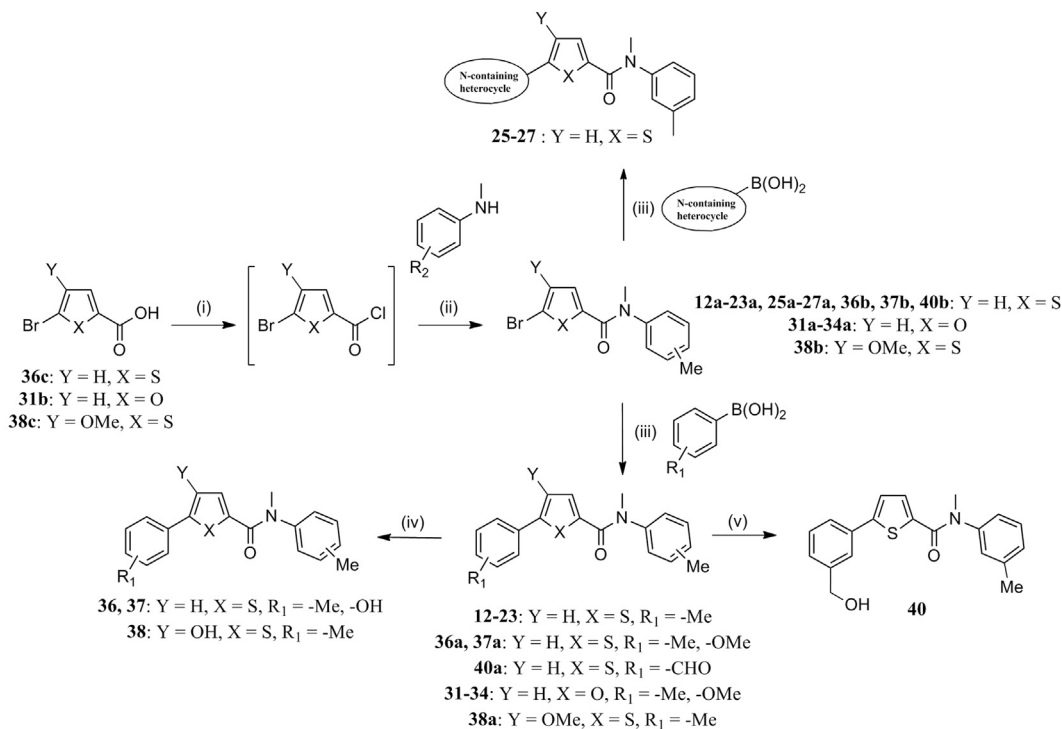
The best 17β-HSD2 inhibitory potency associated with the best selectivity over 17β-HSD1 was achieved for compounds with the C



source according to described methods [37–39]. Inhibitory activities of compounds **12–40** are shown in Tables 2–5, either as IC₅₀ values or as percent of inhibition values determined at 1 μM. Compounds showing less than 10% inhibition at this concentration were considered to be inactive.

ring bearing a methyl in *meta* position while on ring A the methyl can be in either in *meta* or *para* position (compounds **12** and **13**, IC₅₀ = 52 nM and 58 nM; s.f. = 83 and 66, respectively). The selectivity factor is slightly decreased in comparison to the reference compounds **1** and **2**. Compound **14** with the methyl on the C ring in *meta* position and the methyl on the A ring in *ortho* position shows significantly decreased 17β-HSD2 inhibitory potency (IC₅₀ = 715, s.f. = 7), indicating that the geometry of the A ring is critical for activity.

Substitution of the C ring with a methyl in *ortho* position, together with the A ring being either *para* or *meta* methyl substituted, leads to a slight decrease in 17β-HSD2 inhibitory potency and to an increase in 17β-HSD1 inhibition, providing compounds with a poor selectivity factor (compounds **15** and **16**, IC₅₀ = 380 nM and 225 nM and s.f. = 3 and 3, respectively). If both A and C rings are *ortho* substituted, 17β-HSD2 and 17β-HSD1 activity are strongly decreased (compound **17**, 14% inhibition and no inhibition for 17β-HSD2 and 17β-HSD1 at 1 μM, respectively).



^aReagents and conditions: (i) SOCl₂, DMF cat., toluene, reflux 4 h; (ii) Et₃N, CH₂Cl₂, room temperature, overnight; (iii) DME/EtOH/H₂O (1:1:1), Cs₂CO₃, Pd(PPh₃)₄, microwave irradiation (150°C, 150W, 20 min); (iv) BF₃·SMe₂, CH₂Cl₂, room temperature, overnight; (v) NaBH₄, MeOH/Dioxane (1:1), 0 °C, 2 h.

Scheme 1. Synthesis of 2,5-thiophene derivatives **12–23**, **25–27**, **36–38** and **40** and 2,5-furane derivatives **31–34**.^a

Substitution of the C ring with a methyl group in *para* position in combination with a *meta* or *para* substituted A ring led to compounds with moderately decreased 17 β -HSD2 inhibition and decreased selectivity over 17 β -HSD1 (compounds **18** and **19**, IC₅₀ = 892 nM and 772 nM, s.f. = 3 and 2, respectively). *Ortho* substitution of the A ring coupled with *para* substitution of the C ring, surprisingly leads to an inversion of selectivity (compound **20**, 26% and 50% inhibition of 17 β -HSD2 and 17 β -HSD1 at 1 μ M, respectively).

In the 2,5-thiophene class the highest inhibition is observed for a compound showing an *m,p*-dimethyl substitution on the A ring and a *meta* methyl substitution on the C ring (compound **21**, IC₅₀ = 33 nM, s.f. = 352), indicating that the positive effect on the activity of the two methyl groups on the A ring is additive. Furthermore, the presence of the two methyl groups increases the selectivity over 17 β -HSD1. Compound **21** turns out to be the most active and selective compound in this class.

The exchange of the methyl in *meta* position on either the A or the C ring with a chlorine decreases both 17 β -HSD2 inhibitory potency and selectivity over 17 β -HSD1 (compounds **22** and **23**, IC₅₀ = 327 nM and 474 nM, s.f. = 29 and 5, respectively). The importance of the molecular electrostatic potential (MEP) for the ability of 17 β -HSD2 and 17 β -HSD1 inhibitors to establish a π -stacking interaction with aromatic amino acids from the active site has been recently discussed [40]. The decrease in the 17 β -HSD2 inhibition of compounds **22** and **23** can be explained by the difference in the MEPs of the two aromatic rings, elicited by the exchange of the methyl group with a chlorine. This exchange on the A ring seems to be favorable for the 17 β -HSD1 inhibitory potency (compound **23**, IC₅₀ = 2144 nM for 17 β -HSD1).

The introduction of lipophilic substituents on ring A and C increases cLogP values for compounds **12–23** slightly compared to **1**

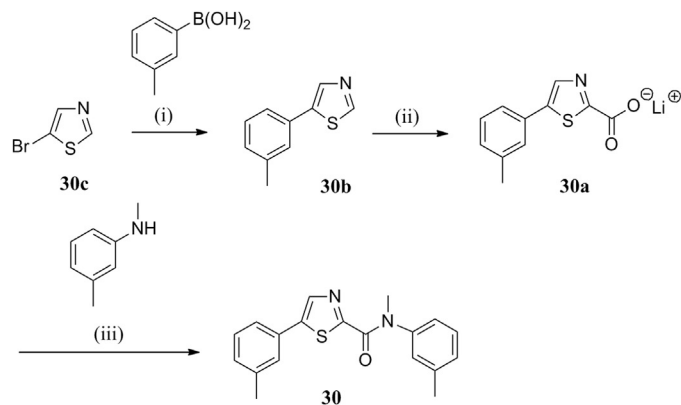
and **2** (Table 2). However, the values are still below 5, which should be sufficient for an acceptable bioavailability [41]. Since lipophilic compounds are usually more susceptible to phase I metabolism [35], in a second step we tried to lower cLogP of the 2,5-thiophene derivatives by exchanging the methylphenyl A ring for different heterocycles like 2-methylpyridinyl **25**, 3-methylpyridinyl **26** or 1-methyl-1H-pyrazolyl **27** (Table 3).

The calculated LogP values of compounds **25**, **26** and **27** are lower and therefore advantageous for their bioavailability compared to the one of compound **12** (3.38, 3.45 and 2.46 for **25**, **26** and **27**, respectively, 4.77 for **12**, Tables 2 and 3).

However the exchange of the A ring with these heterocycles led to a strong decrease in activity (compounds **25**, **26** and **27**: 18%, 28% and 16% inhibition at 1 μ M, respectively). Once again the change in the MEP of the A ring might be responsible for this decreased activity.

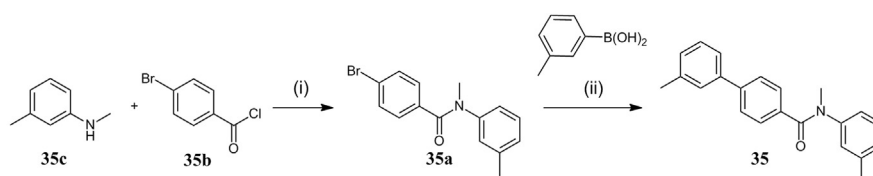
As the methyl substituents on rings A and C in the 2,5-thiophene class were discovered to be very well tolerated by 17 β -HSD2, especially in *meta* position, and to induce a good selectivity over 17 β -HSD1 they will be maintained for the subsequent modifications.

3.2.1.2. Influence of the central core. In a previous study [42], the central 2,5-thiophene-carboxamide of **2** was replaced by a thiazole-2-carboxamide and by a thiazole-5-carboxamide (compounds **28** and **29**, IC₅₀ values 296 nM and 621 nM, s.f. = 63 and 8, respectively, Table 4). Comparison of the potency of **28** and **29**, indicates that the thiazole-2-carboxamide is better in terms of 17 β -HSD2 inhibition and selectivity over 17 β -HSD1 in presence of a methoxy group in position 3 on the C ring. As we had experienced that in the 2,5-thiophene class the methoxy group can be replaced by a methyl (compound **12**) we decided to synthesize the thiazole-2-



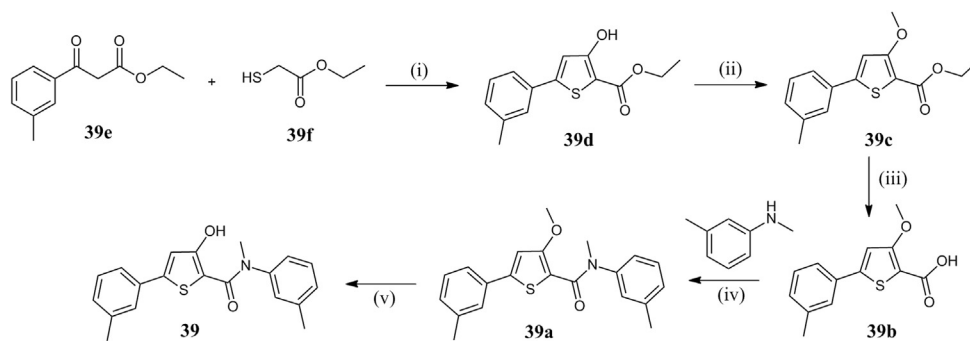
^aReagents and conditions: (i) DME/EtOH/H₂O (1:1:1), Cs₂CO₃, Pd(PPh₃)₄, microwave (150°C, 150 W, 15 min); (ii) a) dry THF, *n*-BuLi, -78°C to 0°C, 4 h, b) dry CO₂ gas, -78°C, 5 h, room temperature, overnight; (iii) a) oxalyl chloride, DMF cat., CH₂Cl₂, 3 h, b) Et₃N, CH₂Cl₂, room temperature, overnight.

Scheme 2. Synthesis of compound **30**.^a



^aReagents and conditions: (i) Et₃N, CH₂Cl₂, room temperature, overnight; (ii) DME/EtOH/H₂O (1:1:1), Cs₂CO₃, Pd(PPh₃)₄, microwave irradiation (150°C, 150W, 20 min).

Scheme 3. Synthesis of compound **35**.^a



^aReagents and conditions: (i) a) HCl(g), room temperature, 5 h, b) NaOEt, room temperature, 2h; (ii) MeI, K₂CO₃, acetonitrile, reflux, 48 h; (iii) KOH, H₂O/THF (1:1), reflux, 4 h; (iv) a) SOCl₂, DMF cat., toluene, reflux 4 h, b) Et₃N, CH₂Cl₂, room temperature, overnight; (v) BF₃·SMe₂, CH₂Cl₂, room temperature, overnight.

Scheme 4. Synthesis of compound **39**.^a

carboxamide with a methyl group on the A and C ring (compound **30**, IC₅₀ = 499 nM, s.f. = 51). This structure modification leads to a 2-fold decrease in activity compared to compound **28**, indicating that as observed in the 2,5-thiophene class, no crucial interaction is achieved by the oxygen atom of the methoxy group.

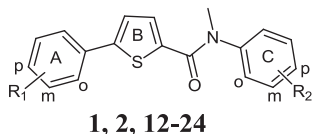
In addition the introduction of the methyl substituent in the thiazole-2-carboxamides did not sufficiently improve 17β-HSD2 inhibitory potency to make them superior to the 2,5-thiophene amides as already described by us [42].

The replacement of the 2,5-thiophene for a 2,5-furane ring is detrimental for the 17β-HSD2 inhibitory potency as shown by

compounds **31–34**. The strongest inhibition of 17β-HSD2 was achieved by compound **34** (38% inhibition at 1 μM), demonstrating that the furane ring is not a suitable bioisostere for the thiophene in these compounds, in contrast to observations made in other compound classes [43]. The furane is less aromatic than the thiophene (electron rich system) because the electronegativity of the oxygen renders the electron pair on this atom less available for resonance. This makes the furane less suitable for π-stacking interactions. The electrostatic potential of the thiophene and furane derivatives are therefore different which might explain the decrease in the activity associated with the furanes.

Table 2

Inhibition of human 17 β -HSD2 and 17 β -HSD1 by biphenyl-2,5-thiophene amide derivatives **12**–**24** with different substitution patterns on the A and C rings in cell-free systems.



Compd.	R ₁	R ₂	Inhibition		Selectivity factor ^d	cLogP ^e
			IC ₅₀ (nM) ^a or % of inhibition at 1 μ M ^a			
			17 β -HSD2 ^b	17 β -HSD1 ^c		
1	<i>m</i> -OMe	<i>m</i> -OMe	58 nM	6728 nM	116	3.68
2	<i>m</i> -Me	<i>m</i> -OMe	68 nM	7616 nM	112	4.38
12	<i>m</i> -Me	<i>m</i> -Me	52 nM	4306 nM	83	4.77
13	<i>p</i> -Me	<i>m</i> -Me	58 nM	3825 nM	66	4.77
14	<i>o</i> -Me	<i>m</i> -Me	715 nM	4570 nM	7	4.77
15	<i>m</i> -Me	<i>o</i> -Me	380 nM	1177 nM	3	4.77
16	<i>p</i> -Me	<i>o</i> -Me	225 nM	698 nM	3	4.77
17	<i>o</i> -Me	<i>o</i> -Me	14%	ni	nd	4.77
18	<i>m</i> -Me	<i>p</i> -Me	892 nM	2687 nM	3	4.77
19	<i>p</i> -Me	<i>p</i> -Me	772 nM	1562 nM	2	4.77
20	<i>o</i> -Me	<i>p</i> -Me	27%	50%	nd	4.77
21	<i>m</i> -Me, <i>p</i> -Me	<i>m</i> -Me	33 nM	11,576 nM	352	5.23
22	<i>m</i> -Me	<i>m</i> -Cl	327 nM	9412 nM	29	5.03
23	<i>m</i> -Cl	<i>m</i> -Me	474 nM	2144 nM	5	4.87
24	H	H	48%	14%	nd	nd

ni: no inhibition, nd: not determined.

^a Mean value of at least two determinations, standard deviation less than 25%.

^b Human placental, microsomal fraction, substrate E2, 500 nM, cofactor NAD⁺, 1500 μ M.

^c Human placental, cytosolic fraction, substrate E1, 500 nM, cofactor NADH, 500 μ M.

^d IC₅₀(17 β -HSD1)/IC₅₀(17 β -HSD2).

^e Calculated data.

Finally the replacement of the central ring by a 1,4-diphenyl substitution leads to compound **35**, with an IC₅₀ value of 1126 nM and an s.f. of 10. The exchange of the thiophene with a benzene decreases 17 β -HSD2 inhibition moderately. However, in comparison with the furane series, in the benzenes some selectivity over 17 β -HSD1 is sustained (Table 4).

The exchange of the central thiophene ring of **12** (cLogP = 4.77) by thiazole (**30**, cLogP = 4.58) and by furane (**31**–**34**, cLogP = 3.86, 3.17, 3.62 and 4.32, respectively) lowers the cLogP value, whereas it is slightly increased in case of the benzene derivative **35**; (cLogP = 4.93, Table 4). However, all compounds show cLogP values in range, which is acceptable for a good bioavailability according to literature [41].

3.2.2. Hydroxy derivatives of **12** and their precursors

Oxidation often occurs during metabolism and in some cases leads to highly active metabolites. Several oxidation products derived from **12** were synthesized and evaluated for their biological activity in vitro (Table 5).

Introduction of an additional methoxy group in *para* position of compound **12** (*ortho* to methyl) leads to compound **36a** (Table 5) showing a significantly decreased activity (66% inhibition at 1 μ M). A similar loss in activity is observed for the hydroxylated compound **36** (62% inhibition at 1 μ M), indicating that in this position introduction of groups like a methoxy or hydroxy is not well tolerated.

This effect is also observed with the introduction of a second substituent in *meta* position of ring A in compound **12** (Table 5). In fact compound **37a**, bearing an additional methoxy group and compound **37**, with an additional hydroxy group in *meta* position, show a similar inhibitory potency over 17 β -HSD2 but lower than the one of the monomethyl **12** (56% and 53% inhibition at 1 μ M, respectively) or the monomethoxy **1** (IC₅₀ value 58 nM). This result indicates that no additive effect is obtained by addition of both methoxy and methyl group in *meta* position, perhaps due to a steric hindrance.

The introduction of a methoxy group or a hydroxy group in position 4 of the thiophene resulting in compounds **38a** and **38** (59% and 64% inhibition at 1 μ M, respectively) is detrimental for activity. This might be due to conformational effects on the phenyl A ring, steric hindrance in the binding site or repulsion of the polar groups caused by the lipophilic environment in the binding cavity.

On the other hand, a methoxy group in position 3 of the thiophene leading to compound **39a** (Table 5), decreases activity only slightly in comparison to **12** (IC₅₀ = 127 nM and 52 nM, respectively) whereas selectivity is increased (s.f. = 132 and 83, respectively).

Exchanging this methoxy by a hydroxy group (compound **39**) leads to a decreased activity (67% inhibition at 1 μ M, Table 5). This indicates that in position 3 of the thiophene a lipophilic group is tolerated whereas a hydrophilic substituent, such as a hydroxy, is detrimental for activity.

Exchange of the methyl group on ring A of compound **12** by an aldehyde (compound **40a**) or by a CH₂OH group (**40**) decreases inhibitory potency (62% and 55% inhibition at 1 μ M, respectively, Table 5).

3.3. Affinity for the estrogen receptors

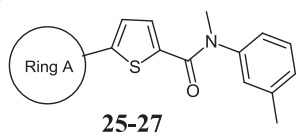
17 β -HSD2 inhibitors should have no affinity for the estrogen receptors (ERs) α and β in order to avoid potential ER mediated side effects. Compounds **12**, **13**, **21**, **22**, **30** and **35** have been tested according to described methods [44] and the results have been expressed in terms of percent [³H]-E2 displaced from the receptor by the inhibitor (Table 6). Shortly, ER α or ER β were incubated with [³H]-E2 and test compound. Subsequently the percent [³H]-E2 displaced from the receptor by the inhibitors was determined, which were tested at concentrations 1000 times higher than the one of [³H]-E2 (Table 6). All inhibitors tested were able to displace less than 50% of [³H]-E2 from the corresponding receptor at this concentration. In terms of Relative Binding Affinity (RBA), their RBA values are <0.1% for both ER α and β , indicating a low binding affinity.

3.4. Metabolic stability in human S9 fraction

We evaluated the most promising inhibitors for metabolic stability using human liver S9 fraction according to described methods [45–47]. Briefly, incubations were run with the S9 fraction, cofactors (for phase I and II reaction) and inhibitor. The concentration of the remaining test compound at the different time points was analyzed by LC-MS/MS and the results expressed as half-lives (*t*_{1/2}) and reported in Table 7.

Exchange of the two methoxy of compound **1** (*t*_{1/2} = 17 min) by two methyl groups provides compound **12** (*t*_{1/2} = 19 min), which is also rather metabolically labile (Table 7). Changing the substitution pattern of the methyl functions does not influence metabolic stability, as it results from comparison of *meta*-, *meta*-**12**, *para*-, *meta*-**13** and *para*-, *ortho*-**16** (*t*_{1/2} = 19 min, 15 min and 22 min, respectively).

Table 3
2,5-Thiophene amides N-containing heterocycle as A ring **25–27**. Inhibition of human 17 β -HSD2 and 17 β -HSD1.



Compd.	Ring A	% Inhibition at 1 μ M ^a		cLogP ^d
		17 β -HSD2 ^b	17 β -HSD1 ^c	
25		18%	n.i.	3.38
26		28%	n.i.	3.45
27		16%	n.i.	2.46

ni: no inhibition.

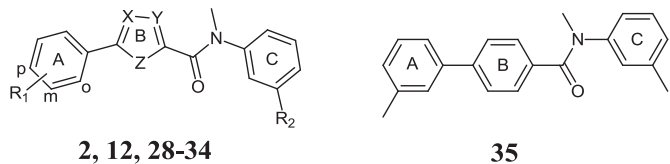
^a Mean value of at least two determinations, standard deviation less than 25%.

^b Human placental, microsomal fraction, substrate E2, 500 nM, cofactor NAD⁺, 1500 μ M.

^c Human placental, cytosolic fraction, substrate E1, 500 nM, cofactor NADH, 500 μ M.

^d Calculated data.

Table 4
Exchange of the central core B. Inhibition of human 17 β -HSD2 and 17 β -HSD1.



Compd.	X	Y	Z	R ₁	R ₂	Inhibition		Selectivity factor ^d	cLogP ^e
						IC ₅₀ (nM) ^a or % of inhibition at 1 μ M ^a			
						17 β -HSD2 ^b	17 β -HSD1 ^c		
2	H	H	S	<i>m</i> -Me	–OMe	68 nM	7616 nM	112	3.68
12	H	H	S	<i>m</i> -Me	–Me	52 nM	4306 nM	83	4.77
28	H	N	S	<i>m</i> -Me	–OMe	296 nM	18,663 nM	63	4.19
29	N	H	S	<i>m</i> -Me	–OMe	621 nM	4821 nM	8	3.91
30	H	N	S	<i>m</i> -Me	–Me	499 nM	25,302 nM	51	4.58
31	H	H	O	<i>m</i> -Me	–Me	14%	31%	nd	3.86
32	H	H	O	<i>m</i> -OMe	–Me	ni	16%	nd	3.17
33	H	H	O	<i>o</i> -F, <i>m</i> -OMe	–Me	34%	26%	nd	3.62
34	H	H	O	<i>m</i> -Me, <i>p</i> -Me	–Me	38%	46%	nd	4.32
35	–	–	–	–	–	1126	11,541	10	4.93

ni: no inhibition, nd: not determined.

^a Mean value of at least two determinations, standard deviation less than 25%.

^b Human placental, microsomal fraction, substrate E2, 500 nM, cofactor NAD⁺, 1500 μ M.

^c Human placental, cytosolic fraction, substrate E1, 500 nM, cofactor NADH, 500 μ M.

^d IC₅₀(17 β -HSD1)/IC₅₀(17 β -HSD2).

^e Calculated data.

Compound **21** ($t_{1/2}$ = 20 min), bearing an additional methyl in *para*-position on ring A, in comparison to **12** does not show an improved stability (**21** $t_{1/2}$ = 20 min vs. **12** $t_{1/2}$ = 19 min).

Compound **22**, with a chlorine on ring C, shows a slightly increased half-life ($t_{1/2}$ = 32 min) in comparison to **12** ($t_{1/2}$ = 19 min).

In addition compound **41**, previously described [25], and bearing a free carboxamide moiety was also tested for stability. In comparison to the others thiophene derivatives and more especially to the methylated analog **5**, it is exceptionally stable ($t_{1/2}$ = 117 min). It is not clear whether the methyl group of the N–CH₃ amide is the metabolic reactive site or whether its absence stabilizes another site in the molecule.

Replacement of the thiophene by a furane (compound **31**, $t_{1/2}$ = 92 min) or by a benzene (compound **35**, $t_{1/2}$ \geq 120 min) results in strong improvement of metabolic stability. On the contrary, exchange of the thiophene by a thiazole leads to very labile compound (**30**, $t_{1/2}$ = 5 min). From these results, it is likely that the thiophene plays a major role in the metabolic fate in the 2,5-thiophene class of compounds.

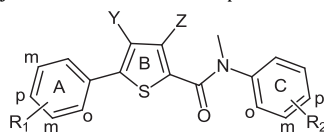
The strategy of lowering the cLogP of compound **12** (cLogP = 4.77), in order to improve the metabolic stability, led to the pyrazole **27** (cLogP = 2.46) and the pyridine **25** (cLogP = 3.38). As expected the most hydrophilic compound **27** ($t_{1/2}$ = 82 min), is more stable than compounds **25** ($t_{1/2}$ = 21 min), and **12** ($t_{1/2}$ = 19 min).

3.5. Metabolites identification

Three compounds (**1**, **2** and **12**) were investigated regarding their metabolic fate and tested in the human S9 fraction using a similar procedure as already described for determination of the metabolic stability. Inhibitors were incubated at a concentration of 10 μ M without phase II cofactors for three hours (no phase II metabolism is expected). After extraction the samples were analyzed using a high resolution LC-MS (LTQ/Orbitrap). Potential metabolites were identified by searching for expected biotransformations (Table 8). The results are presented as area percentage relative to the remaining parent compound. In some cases two different peaks were found for one biotransformation, due to its occurrence at two different sites of the molecule.

For the most prominent metabolites, we propose a structure based on comparison of the fragmentation pattern of the parent compound and the ones of the metabolites (Fig. 1). The spectrum of **1** (Fig. 1(a)) contains strong signals at m/z 136 and 164, representing the substituted aniline ring without or with the amide function, respectively. It also contains the signal m/z 217 representing the left part of the molecule after cleavage of the amide function. This fragmentation is observed in all the tested 2,5-thiophene amide inhibitors and their metabolites. The main metabolite of compound **1** is a demethylated product that accounts for 27% of the remaining parent compound (Table 8). The spectrum of this demethylation product (Fig. 1(b)) still contains the signals m/z 136 and 164, indicating that no demethylation occurred either on the C ring or on the amide. A new signal at m/z 203, coming from the left part of the molecule, indicates that the cleavage of the methoxy occurred on the A ring. In addition a second demethylation product was also observed representing 9% of the remaining parent compound as well as an +O product (12%, Table 8). Other biotransformations result in negligible amounts (Table 8). The exact structure of these metabolites was not identified.

In case of **2** (Fig. 1(c) and (d)) the metabolic demethylation (7% of the remaining parent compound) was less intense compared to the methoxy compound **1**, whereas the +16 biotransformation (Table 8) results in two different products, accounting for 14% and

Table 5Inhibition of human 17 β -HSD2 and 17 β -HSD1 by the possible major metabolite of **12** and its precursors in cell-free systems.**12, 36a-40a, 36-40**

Compd.	Y	Z	R ₁	R ₂	Inhibition		Selectivity factor ^d	cLogP ^e
					IC ₅₀ (nM) ^a or % of inhibition at 1 μ M ^a			
					17 β -HSD2 ^b	17 β -HSD1 ^c		
12	–H	–H	<i>m</i> -Me	<i>m</i> -Me	52 nM	4306 nM	83	4.77
36a	–H	–H	<i>m</i> -Me, <i>p</i> -OMe	<i>m</i> -Me	66%	11%	nd	4.45
36	–H	–H	<i>m</i> -Me, <i>p</i> -OH	<i>m</i> -Me	62%	22%	nd	3.93
37a	–H	–H	<i>m</i> -Me, <i>m</i> -OMe	<i>m</i> -Me	56%	28%	nd	4.43
37	–H	–H	<i>m</i> -Me, <i>m</i> -OH	<i>m</i> -Me	53%	13%	nd	3.94
38a	–OMe	–H	<i>m</i> -Me	<i>m</i> -Me	59%	ni	nd	4.47
38	–OH	–H	<i>m</i> -Me	<i>m</i> -Me	64%	ni	nd	4.00
39a	–H	–OMe	<i>m</i> -Me	<i>m</i> -Me	127 nM	16,732 nM	132	4.36
39	–H	–OH	<i>m</i> -Me	<i>m</i> -Me	67%	24%	nd	4.77
40a	–H	–H	<i>m</i> -CHO	<i>m</i> -Me	62%	ni	nd	3.84
40	–H	–H	<i>m</i> -CH ₂ OH	<i>m</i> -Me	55%	ni	nd	3.39

ni: no inhibition, nd: not determined.

^a Mean value of at least two determinations, standard deviation less than 25%.^b Human placental, microsomal fraction, substrate E2, 500 nM, cofactor NAD⁺, 1500 μ M.^c Human placental, cytosolic fraction, substrate E1, 500 nM, cofactor NADH, 500 μ M.^d IC₅₀(17 β -HSD1)/IC₅₀(17 β -HSD2).^e Calculated data.

5% of the remaining parent compound. Comparing the fragmentation pattern of **2** (Fig. 1(c)) and its main oxidation product (Fig. 1(d)) it can be concluded that the oxygen addition occurs on the thiophene phenyl A ring part of the molecule highlighted with the dotted line (Fig. 1(d)). The structure of the metabolite was not elucidated. Also in this case, the other biotransformations were negligible.

For compound **12**, the main metabolic product derives from an oxidation (Table 8). Two different peaks for the +16 biotransformation can be observed (Table 8), one representing 20% of the remaining parent compound and the other 4%. Demethylation (10%), and oxidation of the –CH₃ into carboxylic acid (5%) are also present. For **12**, the demethylation alone can only occur at the amide function. The transformation demethylation + hydroxylation and the di-hydroxylation were also detected for this compound (Table 8).

Comparing the fragmentation pattern of **12** (Fig. 1(e)) and its main oxidation product (Fig. 1(f)), it can be concluded that the oxygen incorporation occurs on the thiophene phenyl part of the molecule highlighted with the dotted line. Comparing the fragmentation pattern of the –CH₃ to –CO₂H biotransformation in the same way (Fig. 1(g)), it becomes apparent that the carboxylic acid group is on the A ring.

Since we were interested in the identification of the exact hydroxylation site for **12** and since the fragmentation pattern using only the MS/MS data was not conclusive, we synthesized the most probable metabolites. They are represented in Fig. 2.

Compound **36–40** are derived from compound **12** with addition of one hydroxy group in different positions (Fig. 2). The mass +16 (Table 8) observed in our experiment could in theory come from an S-oxidation of the thiophene. The S-oxide thiophene is known to be chemically highly unstable [48] and after synthesis it was rapidly degraded (data not shown). In addition since the procedures for metabolite synthesis and identification require the samples to be

exposed to light at room temperature, able to even accelerate the S-oxide degradation [48], it was concluded that the biotransformation product observed is unlikely to be the thiophene S-oxide.

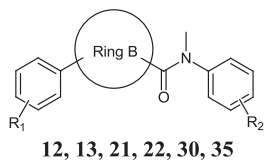
The other 5 potential metabolites, depicted in Fig. 2, were synthesized and co-injected in the LC-MS/MS together with a solution of the metabolites of **12** (Fig. 3).

The chromatograms of the hydroxylated metabolites of **12** alone (Fig. 3(a)) and the one of the co-injection with compound **40** (Fig. 3(b)) are identical with a main peak observed with a retention time of 5.82 min and a minor peak at 6.07 min. The co-injection of any other potential metabolite synthesized (**36–39**) produces spectra with additional peaks having different retention time in comparison to the original spectrum: **36** (Fig. 3(c)), **38** (Fig. 3(d)), **37** (Fig. 3(e)) and **39** (Fig. 3(f)) produce new peaks at 6.25 min, 6.63 min, 6.27 min and 8.03 min, respectively (Fig. 3). This experiment demonstrates the identity of the hydroxylated metabolite of **12** with the hydroxy methyl compound **40**.

To confirm that **40** is the main metabolite of **12** we compared the fragmentation pattern of the metabolite and the synthesized compound (Fig. 4).

As displayed in Fig. 4(a) and (b), the two fragmentation pattern perfectly match. Prominent signals at *m/z* 120, 148, 173 and 217 are present in both spectra. Interestingly, the signal at *m/z* 173 is observed only in the MS2 spectra of **40** and in none of the fragmentation spectra produced for the other potential metabolites (data not shown). This signal is likely to represent the fragment depicted in Fig. 5, derived from the loss of the hydroxy group on the methylene. Since the other potential metabolites all bear an OH directly linked to an aromatic ring (Fig. 2), they might lack the signal at *m/z* 173 because the fragmentation at an aromatic OH needs more energy to be produced. Since this same signal is present in the fragmentation spectrum of the hydroxylated metabolite of compound **2** (Fig. 1(d)) and given the high structural similarity with

Table 6
Percentage of [³H]E2 displaced from the ER α and β for selected compounds.



Compd.	Ring B	R ₁	R ₂	Percentage of [³ H]E2 displaced by the inhibitor ^{a,d}	
				Estrogen receptor α^b	Estrogen receptor β^c
12		<i>p</i> -Me	<i>o</i> -Me	12	21
13		<i>p</i> -Me	<i>m</i> -Me	11	34
21		<i>m</i> -Me, <i>p</i> -Me	<i>m</i> -Me	5	4
22		<i>m</i> -Me	<i>m</i> -Cl	16	11
30		<i>m</i> -Me	<i>m</i> -Me	9	0
35		–	–	8	11

^a Mean value of at least two determinations, standard deviation less than 25%.

^b Recombinant human receptor, ER α 1 nM, [³H]E2 3 nM.

^c Recombinant human receptor, ER β 4 nM, [³H]E2 10 nM.

^d Inhibitor tested at 1000 fold the [³H]E2 concentration, 3 μ M for ER α , 10 μ M for ER β .

12, we could speculate that the hydroxylation reaction occurs at the methyl on the A ring of compound **2** as observed for **12**.

The main metabolic pathway for compound **12** is depicted in Fig. 6. The different metabolites of **12** are expressed both as percentage of the total found metabolites and as percentage of the remaining parent compound in brackets. 39% of the metabolites derives from the hydroxylation of the methyl on the A ring (compound **40**) and its following transformation into a carboxylic acid group (compound **42**) accounts for 10% of the total biotransformations. The cleavage of the methyl on the amide function (compound **43**) represents 19% of all the metabolites and the combination of hydroxylation and demethylation (compound **44**) accounts for 12% of the detected biotransformation products.

4. Discussion

The main goal of this study was the optimization of the metabolic stability of our in house 17 β -HSD2 inhibitors, together with a satisfying understanding of their main routes of metabolism. The new 17 β -HSD2 inhibitors were designed trying to keep potency and selectivity over 17 β -HSD1 and the ERs in an acceptable range while improving their metabolic stability.

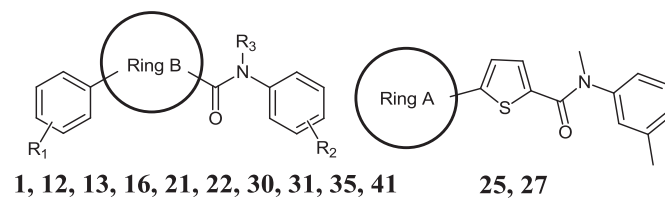
4.1. Potency and selectivity

In the design process we focused on compounds bearing methyl substituents on rings A and C. Compound **12** (IC₅₀ = 52 nM) was obtained, which retains the activity of the dimethoxy analog **1** (IC₅₀ = 58 nM). This result indicates that a polar moiety is not necessary to achieve high potency as previously believed [24],

therefore suggesting that the compounds are not steroidmimetics and do not have the same binding mode as the natural substrate E2.

The effect of all the 9 possible substitution pattern of the methyl groups on rings A and C was studied. The substitution in *meta* or *ortho* position on ring A, while keeping a methyl in *meta* position on ring C (compounds **12** and **13**, IC₅₀ = 52 and 58 nM) leads to an increase in activity of a factor of nearly 20, in comparison with the compound having the two unsubstituted phenyl rings (48% inhibition at 1 μ M) [21]. Recently Leung et al. reported about the effects of the addition of a methyl group to a lead compound on its biological activity, revealing how, from analysis of more than 2000 examples described in the literature, an activity improvement of a factor of 10 or more is found with an 8% frequency only [49]. The authors pointed out that the highest activity increase is often the result from the combination of good fitting of the methyl group into a hydrophobic region of the protein target together with a possible conformational gain, derived from an *ortho* methyl substitution at a

Table 7
Half-life of representative compounds measured in human liver microsomes S9 fraction.



Compd.	Ring B	Ring A	R ₁	R ₂	R ₃	Inhibitor ^c t _{1/2} (min) ^{a,b}
1		–	<i>m</i> -OMe	<i>m</i> -OMe	–Me	17
12		–	<i>m</i> -Me	<i>m</i> -Me	–Me	19
13		–	<i>p</i> -Me	<i>m</i> -Me	–Me	15
16		–	<i>p</i> -Me	<i>o</i> -Me	–Me	22
21		–	<i>m</i> -Me, <i>p</i> -Me	<i>m</i> -Me	–Me	20
22		–	<i>m</i> -Me	<i>m</i> -Cl	–Me	32
41		–	<i>o</i> -F, <i>m</i> -OMe	<i>m</i> -OMe	–H	117
30		–	<i>m</i> -Me	<i>m</i> -Me	–Me	5
31		–	<i>m</i> -Me	<i>m</i> -Me	–Me	92
35		–	–	–	–Me	>120
25	–		–	–	–Me	21
27	–		–	–	–Me	82

^a Extrapolated value. Mean of at least two determinations, standard deviation less than 25%.

^b 1 mg/ml pooled mammalian liver S9 fraction (BD Gentest), 2 mM NADPH regenerating system, 1 mM UDPGA and 0.1 mM PAPS at 37 °C for 0, 5, 15 and 60 min.

^c Inhibitor tested at a final concentration of 1 μ M.

Table 8

List of expected metabolites and their amounts, expressed as area percentage of the remaining parent compound.

Mass difference	Formula	Description	Percentage of metabolite relative to parent compound ^a		
			1	2	12
0	–	Parent	100	100	100
+2	–CH ₂ +O	Demethylation + Hydroxylation	nf	4	6
+16	+O	Hydroxylation, N, S oxidation, epoxidation	12	14	20
+30	+O ₂ –H ₂	CH ₃ to CO ₂ H	nf	nf	5
+32	+O ₂	Di-hydroxylation	2	nf	7
–14	–CH ₂	Demethylation	27	7	10
			9		
–28	–C ₂ H ₄	Didemethylation	2	nf	nf

nf: not found.

^a Area percentage is calculated based on the assumption that each metabolite is equally responsive as parent.

phenyl ring. The increase in inhibitory potency observed in our class of inhibitors might come from the burial of the methyl group in *meta* position on ring A in a hydrophobic pocket of the enzyme, since any conformational restraint induced by *ortho* substitution at this ring (compounds **17** and **20**, 14% and 27% inhibition at 1 μ M, respectively) is detrimental for activity.

By introducing two methyl groups in *para* and *meta* position on ring A, the most potent compound of this class (**21**, IC₅₀ = 33 nM) was obtained, indicating additive effects of the two methyl groups. It also reveals the presence of a likely hydrophobic cavity around ring A.

Exchange of the A ring of compound **12** by different heterocycles like methyl pyridine leads to a significant decrease of activity. This might be due to an unfavorable electrostatic potential of the ring, compared to the phenyl (Table 3) or to the presence of the polar nitrogen, which does not fit well into the enzyme, confirming the presence of a lipophilic cavity. Compound **27**, bearing a 1-methyl-1*H*-pyrazole, is even less potent (Table 3) confirming that polar groups on the A ring are not compatible with a strong binding to the protein target.

The replacement of the central thiophene ring by a furane is also detrimental for activity (**31**, 14% of inhibition at 1 μ M). A small study on the effects of different substituents the A ring resulted in compound **34** as best inhibitor of this series (38% of 17 β -HSD2 inhibition at 1 μ M and 46% of 17 β -HSD1 inhibition at 1 μ M), indicating the inadequateness of this central ring. The furane ring indeed seems to reverse the activity in favor of 17 β -HSD1 inhibition, since **31** and **34** are slightly more active on 17 β -HSD1 and much less active on 17 β -HSD2, in comparison to compound **12** (Table 4).

4.2. Metabolic stability

Compounds **1**, **2** and **3** taken as leads for the study of metabolic stability were found to be rather unstable ($t_{1/2}$ = 17 min, 38 min and 4 min, respectively). An important goal of this work was the improvement of the metabolic stability of this class of compounds. To achieve this goal two different techniques were applied: 1. Modification of the potential reactive site of the inhibitors, 2. Lowering their cLogP.

In order to understand the reason for the instability of **1**, **2** and **3** and in order to identify the metabolically reactive sites in these molecules, a small set of compounds was synthesized and tested. As the methoxy groups seemed to be labile in presence of hepatic enzymes, they were exchanged by methyl groups, in principle slightly more stable. However, this strategy did not improve the

stability of the inhibitors, as seen for compounds **12**, **13**, **22**, **21** and **22** with half-life in the same range as previous molecules ($t_{1/2}$ around 20 min). While replacement of the methoxy group by methyl could preserve inhibitory potency, it did not influence metabolic stability. This can be explained looking at the primary metabolite of **1** and **12**: the methoxy group of **1** as well as the methyl group of **12** on ring A are soon oxidized, thus leading to ether cleavage and CH₂OH formation, respectively. The rate of this reaction, which might be catalyzed by the same enzyme, appears to be in the same order of magnitude for both molecule and the metabolic stability is clearly not influenced by the nature of the substituents on the two compounds.

Given the high structural similarity of compounds **1** and **12** with others 2,5-thiophene amide inhibitors and considering the instability of the tested compounds of this class, it is very likely that the oxidation observed for **1** and **12** is the main metabolic route for the other compounds as well.

Compounds bearing hydroxy groups display half-lives either similar or lower than inhibitors without hydroxy groups (Table 1) and are likely to be also affected by metabolic phase II reactions.

This metabolite identification study clearly indicates that the central thiophene of compound **12** does not constitute a metabolic reactive site and is not susceptible to any biotransformation. Therefore it is striking that the exchange of the thiophene either by a furane or by benzene ring leads to more stable compounds like **31** and **35** ($t_{1/2}$ = 92 min and >120 min, respectively). This means that it is possible to modulate the metabolic rate of compound **12** by modification of the central ring, although it does not constitute a metabolic labile site.

The stability of compound **31** (cLogP = 3.86) might be explained by the decrease in cLogP accomplished by the furane ring in comparison to the thiophene derivative **12** (cLogP = 4.77). This result is also confirmed by the 1-methyl-1*H*-pyrazole compound **27** (cLogP = 2.46) which shows a half-life in human liver S9 fraction of 82 min. Exchange of the thiophene by a benzene ring does not significantly modify the cLogP for **35** (cLogP = 4.93). The improvement in the $t_{1/2}$ of this compound might be caused by a decreased affinity for the metabolizing enzyme, due to a higher steric hindrance.

4.3. Conclusion

In the drug discovery process it is important to take into account the metabolic properties of lead compounds as early as possible. The design of metabolically stable molecules, which maintain the pharmacological activity, is a challenging task. In this work we identified the metabolic liability of a series of 2,5-thiophene amide inhibitors. We have also detailed the specific metabolic pathway of compound **12** and profiled the metabolic fate of **1** and **2**, leading to an overall comprehension of the metabolic liabilities of the 2,5-thiophene amide class of inhibitors. Using two different strategies we discovered three new inhibitors with a highly improved metabolic stability: **27** ($t_{1/2}$ = 82 min), **31** ($t_{1/2}$ = 92 min) and **35** ($t_{1/2}$ = >120 min). The inhibitory potency and selectivity profiles of the synthesized compounds were also evaluated.

Among the three most stable inhibitors, **35** also retains a good activity and selectivity (IC₅₀ = 1126 nM, *s.f.* = 10) and shows no affinity for the estrogen receptors. The relative structural simplicity of compound **35** still leaves room for an appropriate molecular optimization.

5. Experimental section

5.1. Chemical methods

Chemical names follow IUPAC nomenclature. Starting materials were purchased from Aldrich, Acros, Combi-Blocks, Enamine or Fluka and were used without purification.

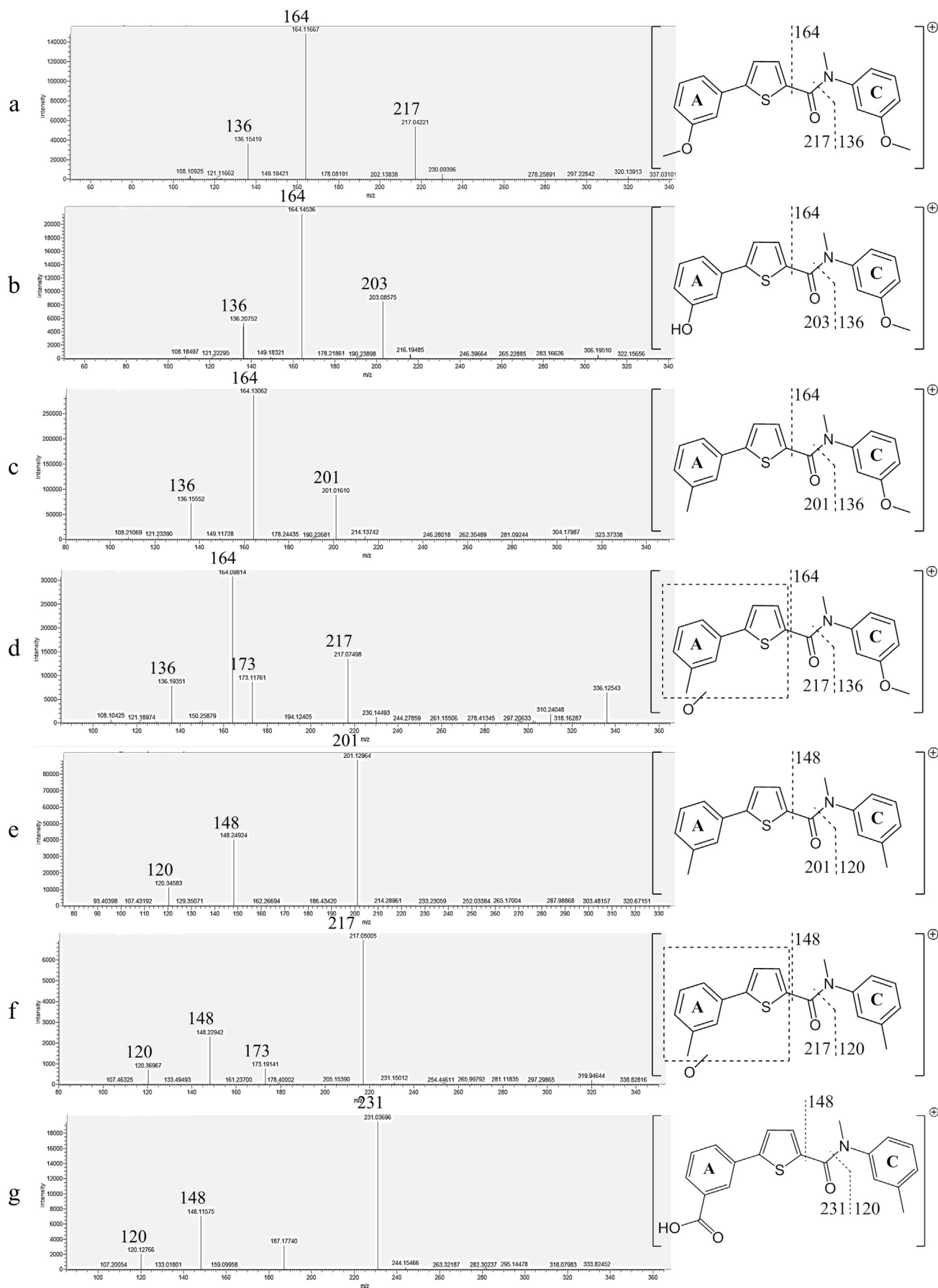


Fig. 1. MS2 spectra of a) **1**; b) **1** major demethylation product; c) **2**; d) **2** major oxidation product; e) **12**; d) **12** oxidation product; g) **12** CH₃ to CO₂H with proposed structures.

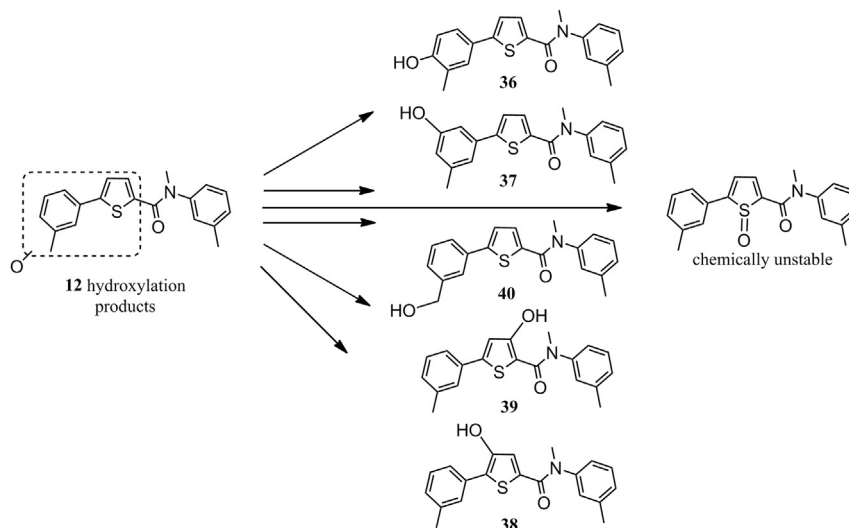


Fig. 2. Potential oxidized metabolites of compound 12.

Column chromatography was performed on silica gel (70–200 μm) and reaction progress was monitored by TLC on Alugram SIL G/UV254 (Macherey–Nagel). Visualization was accomplished with UV light.

^1H NMR and ^{13}C NMR spectra were measured on a Bruker AM500 spectrometer (at 500 MHz and 125 MHz, respectively) at 300 K and on Bruker Fourier 300 (at 300 MHz and 75 MHz, respectively) at 300 K. Chemical shifts are reported in δ (parts per million: ppm), by reference to the hydrogenated residues of deuterated solvent as internal standard: 2.05 ppm (^1H NMR) and 29.8 and 206.3 ppm (^{13}C NMR) for CD_3COCD_3 , 7.26 ppm (^1H NMR) and 77.0 ppm (^{13}C NMR) for CDCl_3 . Signals are described as br (broad), s (singlet), d (doublet), t (triplet), dd (doublet of doublets), ddd (doublet of doublet of doublets), dt (doublet of triplets) and m (multiplet). All coupling constants (J) are given in Hertz (Hz).

Melting points (mp) were measured in open capillaries on a Stuart Scientific SMP3 apparatus and are uncorrected.

Mass spectrometry was performed on a TSQ[®] Quantum (ThermoFisher, Dreieich, Germany). The triple quadrupole mass spectrometer was equipped with an electrospray interface (ESI). The purity of the compounds was assessed by LC/MS. The Surveyor[®]-LC-system consisted of a pump, an auto sampler, and a PDA detector. The system was operated by the standard software Xcalibur[®]. An RP C18 NUCLEODUR[®] 100-5 (3 mm) column (Macherey–Nagel GmbH, Düren, Germany) was used as stationary phase. All solvents were HPLC grade. In a gradient run the percentage of acetonitrile (containing 0.1% trifluoroacetic acid) was increased from an initial concentration of 0% at 0 min to 100% at 15 min and kept at 100% for 5 min. The injection volume was 15 μL and flow rate was set to 800 $\mu\text{L}/\text{min}$. MS analysis was carried out at a needle voltage of 3000 V and a capillary temperature of 350 $^\circ\text{C}$. Mass spectra were acquired in positive mode from 100 to 1000 m/z and UV spectra were recorded at the wave length of 254 nm and in some cases at 360 nm.

All microwave irradiation experiments were carried out in a 507 CEM-Discover microwave apparatus.

All tested compounds exhibited $\geq 95\%$ chemical purity as measured by LC/MS, after dissolving them in methanol.

The following compounds were prepared according to previously described procedures: 5-bromo-*N*-methyl-*N*-(3-methylphenyl)thiophene-2-carboxamide **12a** [25], lithium 5-(3-methylphenyl)-1,3-thiazole-2-carboxylate **30a** [42].

5.1.1. Method A, general procedure for amide formation

A mixture of bromo-*N*-heteroarylcarboxylic acid (2 mmol), thionyl chloride (4 mmol) and DMF (5 drops) in toluene (10 mL) was refluxed at 110 $^\circ\text{C}$ for 4 h. The reaction mixture was cooled to room temperature; the solvent and the excess of thionyl chloride were removed under reduced pressure. The corresponding *N*-methylamine (2 mmol) and Et_3N (2 mmol) in CH_2Cl_2 (10 mL) was added at 0 $^\circ\text{C}$ under N_2 atmosphere to the acyl chloride. After 30 min at 0 $^\circ\text{C}$, the ice bath was removed and the solution was warmed up and stirred at room temperature overnight. The reaction mixture was extracted twice with CH_2Cl_2 (2×15 mL); the organic layer was dried over MgSO_4 , filtered and the solution was concentrated under reduced pressure. The residue was purified by silica gel column chromatography using *n*-hexane and EtOAc as eluent or by trituration in a mixture of diethyl ether/petroleum ether to afford the desired compound.

5.1.2. Method B, general procedure for Suzuki–Miyaura coupling

In a sealed tube the previously prepared bromo-*N*-heteroarylcarboxamide derivative (1 eq.) was introduced followed by the corresponding boronic acid (1.5 eq.), cesium carbonate (3 eq.), tetrakis(triphenylphosphine)palladium (0.02 eq.) and a mixture of DME/EtOH/ H_2O (1:1:1, v:v:v, 3 mL) as solvent. The reactor was flushed with N_2 and submitted to microwave irradiation (150 $^\circ\text{C}$, 150 W) for 20 min. After cooling to room temperature, a mixture of EtOAc/ H_2O (1:1, v:v, 2 mL) was added to stop the reaction. The aqueous layer was extracted with EtOAc (3×10 mL). The organic layer was washed once with brine and once with water, dried over MgSO_4 , filtered and the solution was concentrated under reduced pressure. The residue was purified by column chromatography using *n*-hexane and EtOAc as eluent to afford the desired compound.

5.1.3. Detailed synthesis procedures of the most interesting compounds

5.1.3.1. *N*-Methyl-*N*,5-bis(3-methylphenyl)thiophene-2-carboxamide (12). The title compound was prepared by reaction of 5-bromo-*N*-methyl-*N*-(3-methylphenyl)thiophene-2-carboxamide **12a** (150 mg, 0.48 mmol), *m*-tolyl boronic acid (86 mg, 0.63 mmol), cesium carbonate (469 mg, 1.44 mmol) and tetrakis(triphenylphosphine) palladium (11 mg, 0.02 eq) according to method B. The residue was purified by silica gel column

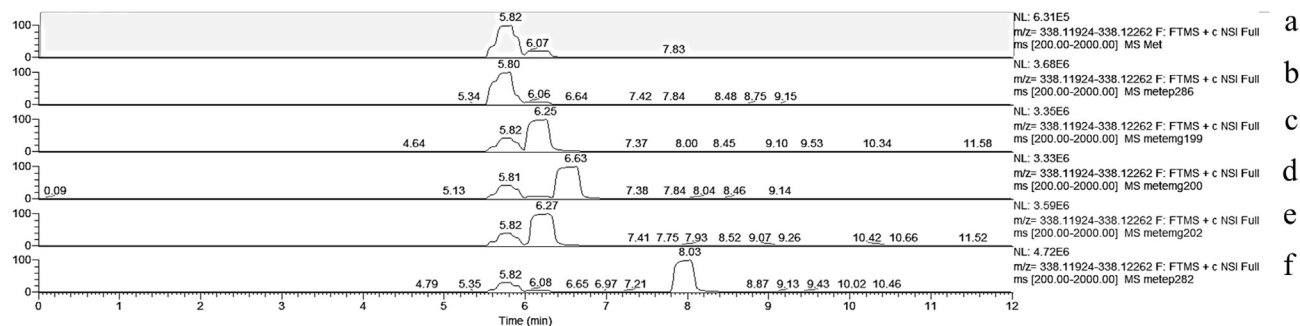


Fig. 3. Ion chromatogram of **12** major oxidation product and its co-injection with the synthesized potential metabolite. On the top of the peaks, the retention times are shown. From the top to the bottom are displayed the six chromatograms of the a) hydroxylation products after incubation with the S9 fraction; b) co-injected with **40**; c) co-injected with **36**; d) co-injected with **38**; e) co-injected with **37**; f) co-injected with **39**.

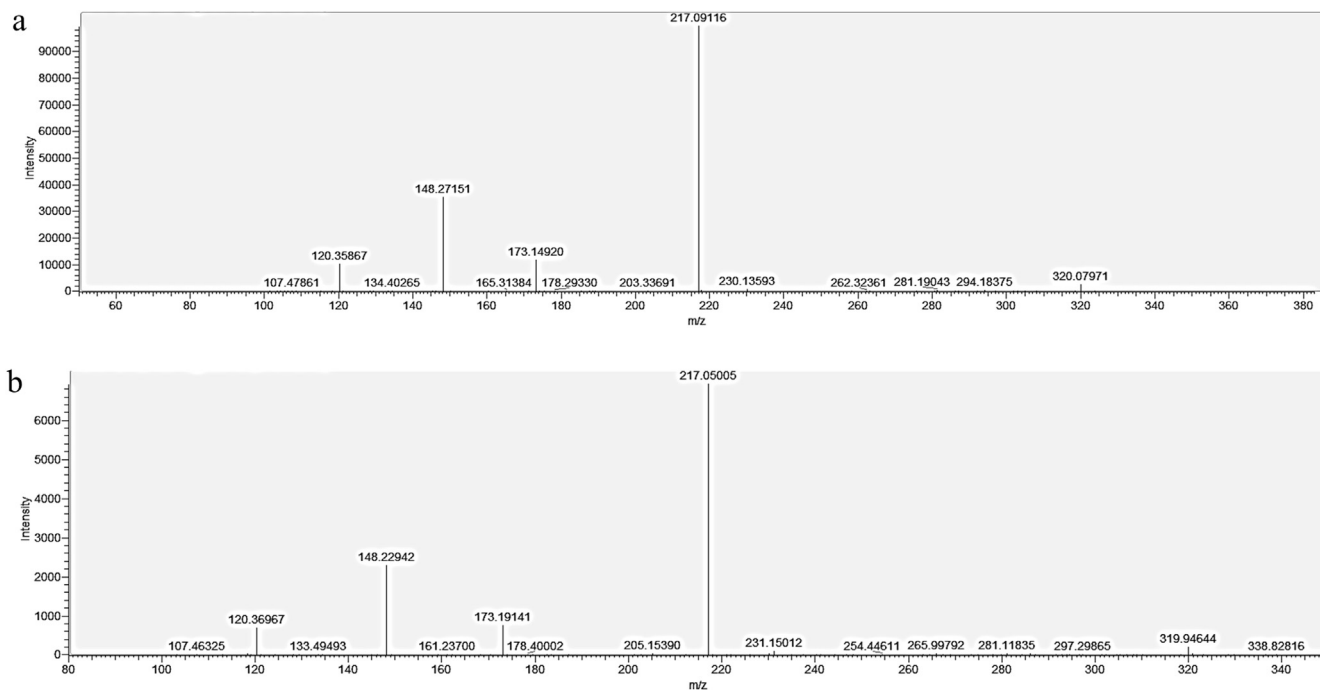


Fig. 4. a) Fragmentation pattern of the pure **40**; b) fragmentation pattern of **12** major hydroxylated product.

chromatography (*n*-hexane/ethyl acetate 80:20) to afford the desired product as yellow solid (117 mg, 76%). $C_{20}H_{19}NOS$; MW 321; mp: 98–101 °C; MS (ESI) 322 $[M+H]^+$; 1H NMR ($CDCl_3$, 500 MHz) 2.36 (s, 3H), 2.39 (s, 3H), 3.47 (s, 3H), 6.68 (d, $J = 4.1$ Hz, 1H), 6.97 (d, $J = 4.1$ Hz, 1H), 7.09–7.12 (m, 3H), 7.21–7.25 (m, 2H), 7.28–7.29 (m, 1H), 7.31–7.34 (m, 2H); ^{13}C NMR ($CDCl_3$, 125 MHz) δ 21.3, 21.4, 39.4, 122.7, 123.2, 125.0, 126.7, 128.5, 128.9, 129.2, 129.7, 133.4, 133.5, 136.3, 138.6, 140.0, 143.8, 149.7, 163.1; IR (cm^{-1}) 3048, 2921, 1599, 1584.

5.1.3.2. *N*-Methyl-*N*-(3-methylphenyl)-5-(4-methylphenyl)thiophene-2-carboxamide (13**).** The title compound was prepared by reaction of 5-bromo-*N*-methyl-*N*-(3-methylphenyl)thiophene-2-carboxamide **12a** (100 mg, 0.32 mmol), *p*-tolyl boronic acid (65 mg, 0.48 mmol), cesium carbonate (313 mg, 0.96 mmol) and tetrakis(triphenylphosphine) palladium (8 mg, 0.02 eq) according to method B. The residue was purified by silica gel column chromatography (*n*-hexane/ethyl acetate 80:20) to afford the desired product as yellow solid (63 mg, 61%). $C_{20}H_{19}NOS$; MW 321; mp: 95–98 °C; MS (ESI) 322 $[M+H]^+$; 1H NMR (CD_3COCD_3 , 500 MHz)

2.32 (s, 3H), 2.36 (s, 3H), 3.37 (s, 3H), 6.49 (d, $J = 3.9$ Hz, 1H), 7.07 (d, $J = 3.9$ Hz, 1H), 7.14–7.16 (m, 1H), 7.19–7.22 (m, 3H), 7.24–7.26 (m, 1H), 7.35 (t, $J = 7.8$ Hz, 1H), 7.46 (dt, $J = 2.0, 8.3$ Hz, 2H); ^{13}C NMR (CD_3COCD_3 , 125 MHz) δ 21.2, 21.3, 39.1, 123.4, 126.1, 126.6, 129.6, 129.7, 130.5, 130.6, 131.8, 133.3, 138.6, 139.3, 140.8, 145.5, 149.3, 162.5; IR (cm^{-1}) 3050, 2921, 1599, 1585.

5.1.3.3. 5-(3,4-Dimethylphenyl)-*N*-methyl-*N*-(3-methylphenyl)thiophene-2-carboxamide (21**).** The title compound was prepared by reaction of 5-bromo-*N*-methyl-*N*-(3-methylphenyl)thiophene-2-carboxamide **12a** (150 mg, 0.48 mmol), 3,4-dimethylphenyl boronic acid (94.5 mg, 0.63 mmol), cesium carbonate (469 mg,

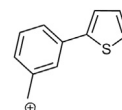


Fig. 5. Proposed structure for signal at m/z 173.

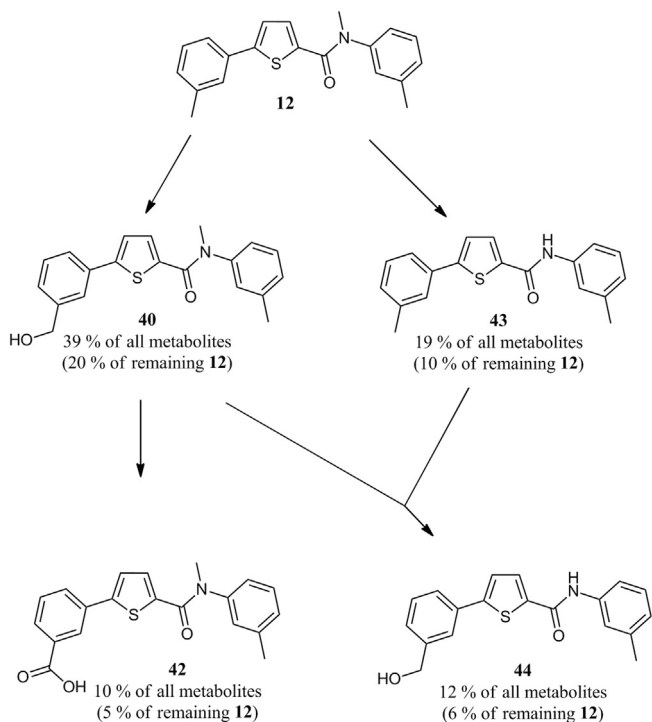


Fig. 6. Proposed pathway for the phase I metabolism of 12 in human S9 fraction.

1.44 mmol) and tetrakis(triphenylphosphine) palladium (11 mg, 0.02 eq) according to method B. The residue was purified by silica gel column chromatography (*n*-hexane/ethyl acetate 80:20) to afford the desired product as colorless solid (55 mg, 34%). $C_{21}H_{21}NOS$; MW 335; mp: 138–140 °C; MS (ESI) 336 [M+H]⁺; ¹H NMR (CDCl₃, 500 MHz) 2.26 (s, 3H), 2.27 (s, 3H), 2.38 (s, 3H), 3.45 (s, 3H), 6.57 (d, *J* = 4.0 Hz, 1H), 6.92 (d, *J* = 4.0 Hz, 1H), 7.08–7.11 (m, 3H), 7.20–7.21 (m, 1H), 7.23 (dd, *J* = 2.1, 7.8 Hz, 1H), 7.28–7.33 (m, 2H); ¹³C NMR (CDCl₃, 125 MHz) δ 19.5, 19.7, 21.3, 39.1, 122.2, 123.4, 125.0, 127.2, 128.5, 128.9, 129.6, 130.1, 131.2, 132.8, 136.6, 137.0, 137.1, 139.8, 144.1, 149.4, 162.6; IR (cm⁻¹) 3029, 2918, 1612, 1602.

5.1.3.4. *N*-Methyl-*N*-(3-methylphenyl)-5-(1-methyl-1*H*-pyrazol-4-yl) thiophene-2-carboxamide (27). The title compound was prepared by reaction of 5-bromo-*N*-methyl-*N*-(3-methylphenyl)thiophene-2-carboxamide 12a (150 mg, 0.48 mmol), 1-methyl-1*H*-pyrazole-4-boronic acid (96 mg, 0.63 mmol), cesium carbonate (626 mg, 1.92 mmol) and tetrakis(triphenylphosphine) palladium (11 mg, 0.02 eq) according to method B. The residue was purified by silica gel column chromatography (*n*-hexane/ethyl acetate 70:30) to afford the desired product as yellow solid (70 mg, 53%). $C_{17}H_{17}N_3OS$; MW 311; mp: 132–134 °C; MS (ESI) 312 [M+H]⁺; ¹H NMR (CDCl₃, 500 MHz) 2.37 (s, 3H), 3.43 (s, 3H), 3.89 (s, 3H), 6.49 (d, *J* = 4.0 Hz, 1H), 6.70 (d, *J* = 4.0 Hz, 1H), 7.06–7.10 (m, 2H), 7.19–7.21 (m, 1H), 7.30 (t, *J* = 7.7 Hz, 1H), 7.47 (s, 1H), 7.57 (d, *J* = 1.0 Hz, 1H); ¹³C NMR (CDCl₃, 125 MHz) δ 21.6, 29.6, 39.0, 116.4, 122.0, 125.0, 127.4, 128.5, 128.9, 129.5, 132.7, 135.4, 137.0, 140.0, 140.2, 144.1, 162.4; IR (cm⁻¹) 3075, 2923, 2854, 1616, 1601, 1582.

5.1.3.5. *N*-Methyl-*N*,5-bis(3-methylphenyl)-1,3-thiazole-2-carboxamide (30). To a solution of lithium 5-(3-methylphenyl)-1,3-thiazole-2-carboxylate 30a (100 mg, 0.44 mmol) in CH₂Cl₂ (15 mL) was added drop wise oxalyl chloride (80 μL, 0.88 mmol) followed by few drops of DMF at 0 °C under N₂ atmosphere. The reaction mixture was stirred at 0 °C for 10 min and then at room

temperature for 3 h. The solvent was removed under reduced pressure (bath temperature of rotavapor at 20 °C). This residue was diluted in dry CH₂Cl₂ (10 mL) and *N*,3-dimethylaniline (0.06 mL, 0.44 mmol) was added followed by triethylamine (0.10 μL, 0.44 mmol). The solution was stirred overnight at room temperature under N₂ atmosphere. The solvent was removed under reduced pressure (bath temperature of rotavapor at 20 °C). A mixture of Na₂CO₃ 2N (15 mL) and EtOAc (15 mL) were added. The aqueous layer was extracted with EtOAc (15 mL). The organic layer was washed twice with Na₂CO₃ 2N (15 mL), once with water (15 mL), dried over MgSO₄, filtered and the solution was concentrated under reduced pressure. The residue was purified by silica gel column chromatography (*n*-hexane/ethyl acetate 70:30) to afford the desired product as pale brown solid (51 mg, 36%). $C_{19}H_{18}N_2OS$; MW 322; mp: 79–80 °C; MS (ESI) 323 [M+H]⁺; ¹H NMR (CDCl₃, 500 MHz) 2.32 (s, 3H), 2.36 (s, 3H), 3.54 (br s, 3H), 7.07–7.09 (m, 1H), 7.10–7.12 (m, 1H), 7.15 (br s, 1H), 7.20–7.26 (m, 1H), 7.32 (t, *J* = 7.7 Hz, 1H), 7.44–7.46 (m, 2H), 7.49 (br s, 1H), 7.93 (br s, 1H); ¹³C NMR (CDCl₃, 125 MHz) 21.3, 39.6, 124.9, 125.0, 128.3, 128.4, 128.6, 130.0, 130.1, 130.6, 131.5, 139.69, 139.70, 139.9, 144.2, 145.4, 161.2. IR (cm⁻¹) 3096, 2922, 1624, 1606, 1585.

5.1.3.6. *N*-Methyl-*N*,5-bis(3-methylphenyl)furan-2-carboxamide (31). The title compound was prepared by reaction of 31a (150 mg, 0.51 mmol), *m*-tolyl boronic acid (104 mg, 0.77 mmol), cesium carbonate (499 mg, 1.53 mmol) and tetrakis(triphenylphosphine) palladium (12 mg, 0.02 eq) according to method B. The residue was purified by silica gel column chromatography (*n*-hexane/ethyl acetate 70:30) to afford the desired product as orange oil (100 mg, 64%). $C_{20}H_{19}NO_2$; MW 305; MS (ESI) 306 [M+H]⁺; ¹H NMR (CD₃COCD₃, 500 MHz) 2.30 (s, 3H), 2.38 (s, 3H), 3.37 (s, 3H), 6.67 (d, *J* = 3.7 Hz, 1H), 6.74 (d, *J* = 3.7 Hz, 1H), 7.00–7.01 (m, 1H), 7.07–7.12 (m, 2H), 7.16–7.22 (m, 3H), 7.24–7.27 (m, 1H), 7.35 (t, *J* = 7.8 Hz, 1H); ¹³C NMR (CD₃COCD₃, 125 MHz) δ 21.3, 38.7, 107.1, 119.4, 122.3, 125.3, 125.4, 128.8, 129.0, 129.5, 129.9, 130.2, 130.7, 139.2, 140.3, 145.9, 148.2, 155.8, 159.1.

5.1.3.7. *N*,3'-Dimethyl-*N*-(*m*-tolyl)-[1,1'-biphenyl]-4-carboxamide (35). The title compound was prepared by reaction of 35a (120 mg, 0.39 mmol), *m*-tolyl boronic acid (69 mg, 0.51 mmol), cesium carbonate (381 mg, 1.17 mmol) and tetrakis(triphenylphosphine) palladium (9 mg, 0.02 eq) according to method B. The residue was purified by silica gel column chromatography (*n*-hexane/ethyl acetate 80:20) to afford the desired product as yellow oil (105 mg, 85%). $C_{22}H_{21}NO$; MW 315; MS (ESI) 316 [M+H]⁺; ¹H NMR (CD₃COCD₃, 300 MHz) 2.24 (s, 3H), 2.37 (s, 3H), 3.42 (s, 3H), 6.93–6.96 (d, *J* = 9 Hz, 1H), 6.98–7.00 (d, *J* = 7 Hz, 1H), 7.07 (s, 1H), 7.11–7.18 (m, 2H), 7.30 (t, *J* = 8 Hz, 1H), 7.37–7.42 (m, 4H), 7.47–7.50 (m, 2H); ¹³C NMR (CD₃COCD₃, 75 MHz) 21.2, 21.4, 38.5, 124.8, 125.1, 126.8, 127.9, 128.4, 128.44, 129.3, 129.6, 129.7, 130.1, 136.5, 139.3, 139.9, 140.8, 142.7, 146.2, 170.2. IR (cm⁻¹) 3037, 2920, 2862, 1740, 1639, 1603.

5.1.3.8. 5-[3-(Hydroxymethyl)phenyl]-*N*-methyl-*N*-(3-methylphenyl) thiophene-2-carboxamide (40). To a solution of 5-(3-formylphenyl)-*N*-methyl-*N*-(3-methylphenyl)thiophene-2-carboxamide 40a (76 mg, 0.23 mmol) in a mixture of dry MeOH (3 mL) and dry dioxane (3 mL) was added at 0 °C sodium borohydride (87 mg, 0.46 mmol). After 2 h at 0 °C, water was added to quench the reaction. The aqueous layer was extracted three times with EtOAc (3 × 5 mL). The organic layer was washed once with saturated solution of NaHCO₃ and once with water, dried over MgSO₄, filtered and the solution was concentrated under reduced pressure. The residue was purified by preparative HPLC (using acetonitrile/water from 10% to 95% of acetonitrile) to afford the

desired product as colorless oil (14 mg, 18%). C₂₀H₁₉NO₂S; MW 337; MS (ESI) 338 [M+H]⁺; ¹H NMR (CDCl₃, 300 MHz) 2.36 (s, 3H), 3.43 (s, 3H), 4.70 (s, 2H), 6.57 (d, *J* = 4.0 Hz, 1H), 6.96 (d, *J* = 4.0 Hz, 1H), 7.04–7.06 (m, 1H), 7.06–7.10 (m, 1H), 7.17–7.22 (m, 1H), 7.27–7.36 (m, 3H), 7.40 (dt, *J* = 1.8, 7.2 Hz, 1H), 7.49–7.51 (m, 1H); ¹³C NMR (CDCl₃, 75 MHz) 21.3, 39.1, 65.0, 122.9, 124.5, 125.0, 125.2, 126.8, 128.5, 129.0, 129.1, 129.6, 132.9, 133.9, 137.4, 139.9, 141.7, 144.1, 148.7, 162.6. IR (cm⁻¹): 3397, 3027, 2921, 2865, 1598, 1582.

5.2. logP Determination

The logP values were calculated from ACD/Labs Percepta 2012 Release program. The logarithm of partition constant P (log P) was calculated using the “GALAS” method (Global Adjusted Locally According to Similarity). The program predicts clogP by comparing the molecule with structurally similar molecules where experimental data are known.

5.3. Biological methods

[2,4,6,7-³H]-E2 and [2,4,6,7-³H]-E1 were purchased from Perkin–Elmer, Boston. Quickszint Flow 302 scintillator fluid was bought from Zinsser Analytic, Frankfurt. Other chemicals were purchased from Sigma, Roth or Merck.

5.3.1. 17β-HSD1 and 17β-HSD2 enzyme preparation

Cytosolic (17β-HSD1) and microsomal (17β-HSD2) fractions were obtained from human placenta according to previously described procedures [38,39,50]. Fresh tissue was homogenized and the enzymes were separated by fractional centrifugation at 1000 g, 10,000 g and 150,000 g. The pellet fraction containing the microsomal 17β-HSD2 was used for the determination of 17β-HSD2 inhibition, while 17β-HSD1 was obtained after precipitation with ammonium sulfate from the cytosolic fraction for use of testing of 17β-HSD1 inhibition. Aliquots containing 17β-HSD1 or 17β-HSD2 were stored frozen.

5.3.2. Inhibition of 17β-HSD2 in cell-free assay

Inhibitory activities were evaluated by an established method with minor modifications [37,51,52]. Briefly, the enzyme preparation was incubated with NAD⁺ [1500 μM] in the presence of potential inhibitors at 37 °C in a phosphate buffer (50 mM) supplemented with 20% of glycerol and EDTA 1 mM. Inhibitor stock solutions were prepared in DMSO. Final concentration of DMSO was adjusted to 1% in all samples. The enzymatic reaction was started by addition of a mixture of unlabeled- and [³H]-E2 (final concentration: 500 nM, 0.11 μCi). After 20 min, the incubation was stopped with HgCl₂ and the mixture was extracted with ether. After evaporation, the steroids were dissolved in acetonitrile/water (45:55). E1 and E2 were separated using acetonitrile/water (45:55) as mobile phase in a C18 RP chromatography column (Nucleodur C18, 3 μm, Macherey–Nagel, Düren) connected to an HPLC-system (Agilent 1100 Series, Agilent Technologies, Waldbronn). Detection and quantification of the steroids were performed using a radioflow detector (Berthold Technologies, Bad Wildbad). The conversion rate was calculated according to the following equation: % conversion = (%E1/(%E1 + %E2)) × 100. Each value was calculated from at least three independent experiments.

5.3.3. Inhibition of 17β-HSD1 in cell-free assay

The 17β-HSD1 inhibition assay was performed similarly to the 17β-HSD2 test. The microsomal fraction was incubated with NADH [500 μM], test compound and a mixture of unlabeled- and [³H]-E1 (final concentration: 500 nM, 0.15 μCi) for 10 min at 37 °C. Further

treatment of the samples and HPLC separation was carried out as mentioned above for 17β-HSD2.

5.3.4. Estrogen receptor affinity in a cellular free assay

The binding affinity of selected compounds to ERα and ERβ was determined according to the recommendations of the US Environmental Protection Agency (EPA) by their Endocrine Disruptor Screening Program (EDSP) [44] using recombinant human proteins. Briefly, 1 nM of ERα and 4 nM of ERβ, respectively, were incubated with [³H]-E2 (3 nM for ERα and 10 nM for ERβ) and test compound for 16–20 h at 4 °C.

The potential inhibitors were dissolved in DMSO (5% final concentration). Evaluation of non-specific-binding was performed with unlabeled E2 at concentrations 100-fold of [³H]-E2 (300 nM for ERα and 1000 nM for ERβ). After incubation, ligand-receptor complexes were selectively bound to hydroxyapatite (83.5 g/L in TE-buffer). The bound complex was washed three times and resuspended in ethanol. For radiodetection, scintillator cocktail (Quickszint 212, Zinsser Analytic, Frankfurt) was added and samples were measured in a liquid scintillation counter (1450 LSC & Luminescence Counter, Perkin Elmer).

From these results the percentage of [³H]-E2 displacement by the compounds was calculated. The plot of % displacement versus compound concentration resulted in sigmoidal binding curves. The compound concentrations to displace 50% of the receptor bound [³H]-E2 were determined. Unlabeled E2 IC₅₀ values were determined in each experiment and used as reference. The E2 IC₅₀ values accepted, were 3 ± 20% nM for ERα and 10 ± 20% nM for ERβ.

Relative Binding Affinity was determined by applying the following equation: RBA[%] = (IC₅₀(E2)/IC₅₀(compound)) · 100 [44]. This results in an RBA value of 100% for E2.

After the assay was established and validated, a modification was made to increase throughput. Compounds were tested at concentrations of 1000 · IC₅₀(E2). Compounds with less than 50% displacement of [3H]-E2 at a concentration of 1000 · IC₅₀(E2) were classified as RBA <0.1%.

5.3.5. Metabolic stability in a cell free assay

Compounds **3**, **5**, **7–9**, **12**, **13**, **16**, **21**, **22**, **25**, **27**, **30**, **31**, **35** and **41** were tested according to established method [45–47]. For evaluation of phase I and II metabolic stability 1 μM compound was incubated with 1 mg/ml pooled mammalian liver S9 fraction (BD Gentest), 2 mM NADPH regenerating system, 1 mM UDPGA and 0.1 mM PAPS at 37 °C for 0, 5, 15 and 60 min at a final volume of 100 μL. The incubation was stopped by precipitation of S9 enzymes with 2 volumes of cold acetonitrile containing internal standard. Concentration of the remaining test compound at the different time points was analyzed by LC-MS/MS and used to determine half-life (t_{1/2}).

Compounds **1**, **2**, **4**, **6**, **10** and **11** were tested following a similar procedure with the following changes: 3 μM compound was incubated with 1 mg/ml pooled mammalian liver S9 fraction (IVT, Xenotech or TCS cellworks), 1 mM NADPH regenerating system, 0.75 mM UDPGA and 0.05 mM PAPS at 37 °C for 0, 5, 15 and 45 min.

5.3.6. Metabolite identification in a cell free assay

Compounds **1**, **2** and **12** were incubated at a final concentration of 10 μM with 1 mg/ml pooled mammalian liver S9 fraction (BD Gentest) and 2 mM NADPH regenerating system for three hours (final volume 3 mL). The water phase was extracted with dichloromethane (3 × mL), which was evaporated to dryness at room temperature. The residue was resuspended in 500 μL methanol. Separation of 2 μL sample was accomplished on a Dionex Ultimate 3000 RSLC system using a BEH C18 50 × 2.1 mm, 1.7 μm d_p column (Waters, Germany). Separation was achieved by a linear

gradient from (A) H₂O + 0.1% formic acid (FA) to (B) ACN + 0.1% FA at a flow rate of 600 µL/min and 45 °C. The gradient was initiated by a 0.33 min isocratic step at 5% B, followed by an increase to 95% B in 9 min to end up with a 1 min step at 95% B before reequilibration under the initial conditions. The flow entered the LTQ/Orbitrap (Thermo Scientific, Germany) using the Nanomate Advion Nano-spray ion source (NSI). The Mass Spectrometer was set with the following parameters: scan range 200–2000 *m/z* in positive ionization mode; 200 °C Capillary Temperature; 1.7 kV Voltage at NSI; Fourier Transform Mass Spectrometry (FTMS) Resolution of 30,000; MS/MS analysis was data-dependent and triggered by the most abundant ions.

Data Acquisition was performed with Xcalibur version 1.0.2.65 (Thermo Electron, San Jose, Ca, USA). Five-decimal monoisotopic masses of **1**, **2** and **15** and their predicted metabolites, calculated from CambridgeSoft Chem & Bio Draw 11.0 using the ChemDrawPro 1.0 program, were used for the parent data and to filter data in Qual Browser (Thermo Electron, San Jose, Ca, USA) with a mass tolerance threshold of 5 ppm.

Author contributions

The manuscript was written through contributions of all authors. All authors have given approval to the final version of the manuscript.

Acknowledgment

We thank Josef Zapp for the NMR measurement, Isabella Mang, Theresa Manz and Martina Jankowski for the biological test. We are thankful to Prof. R. Müller for the access to the LTQ/Orbitrap apparatus and Eva Luxemburger for the help in the measurements. We acknowledge the Deutsche Forschungsgemeinschaft (DFG) for financial support (Grants HA1315/12-1 and AD 127/10-1).

Appendix A. Supplementary data

Supplementary data associated with this article can be found in the online version, at <http://dx.doi.org/10.1016/j.ejmech.2014.09.061>. These data include MOL files and InChIKeys of the most important compounds described in this article.

References

- [1] M. Cree, C.L. Soskolne, E. Belseck, J. Hornig, J.E. McElhaney, R. Brant, M. Suarez-Almazor, *J. Am. Geriatr. Soc.* 48 (2000) 283–288.
- [2] L.J. Melton 3rd, E.A. Chrischilles, C. Cooper, A.W. Lane, B.L. Riggs, *J. Bone Miner. Res.* 7 (1992) 1005–1010.
- [3] R. Burge, B. Dawson-Hughes, D.H. Solomon, J.B. Wong, A. King, A. Tosteson, *J. Bone Miner. Res.* 22 (2007) 465–475.
- [4] R. Marcus, M. Wong, H. Heath 3rd, J.L. Stock, *Endocr. Rev.* 23 (2002) 16–37.
- [5] E. Orwoll, M. Ettinger, S. Weiss, P. Miller, D. Kendler, J. Graham, S. Adami, K. Weber, R. Lorenc, P. Pietschmann, K. Vandormael, A. Lombardi, *N. Engl. J. Med.* 343 (2000) 604–610.
- [6] J.D. Ringe, H. Faber, P. Farahmand, A. Dorst, *Rheumatol. Int.* 26 (2006) 427–431.
- [7] B. Ettinger, D.M. Black, B.H. Mitlak, R.K. Knickerbocker, T. Nickelsen, H.K. Genant, C. Christiansen, P.D. Delmas, J.R. Zanchetta, J. Stakkestad, C.C. Glüer, K. Krueger, F.J. Cohen, S. Eckert, K.E. Ensrud, L.V. Avioli, P. Lips, S.R. Cummings, *J. Am. Med. Assoc.* 282 (1999) 637–645.
- [8] P.V.N. Bodine, B.S. Komm, *Vitam. Horm.* 64 (2002) 101–151.
- [9] D.T. Felson, Y. Zhang, M.T. Hannan, D.P. Kiel, P.W. Wilson, J.J. Anderson, *N. Engl. J. Med.* 329 (1993) 1141–1146.
- [10] C.L. Chen, N.S. Weiss, P. Newcomb, W. Barlow, E. White, *J. Am. Med. Assoc.* 287 (2002) 734–741.
- [11] S.A. Beresford, N.S. Weiss, L.F. Voigt, B. McKnight, *Lancet* 349 (1997) 458–461.
- [12] D. Vanderschueren, J. Gaytant, S. Boonen, K. Venken, *Androgens and bone*, *Curr. Opin. Endocrinol. Diabetes Obes.* 15 (2008) 250–254.
- [13] D. Vanderschueren, L. Vandenput, S. Boonen, M.K. Lindberg, R. Bouillon, C. Ohlsson, *Endocr. Rev.* 25 (2004) 389–425.
- [14] L. Wu, M. Einstein, W.M. Geissler, H.K. Chan, K.O. Elliston, S. Andersson, *J. Biol. Chem.* 268 (1993) 12964–12969.
- [15] S. Marchais-Oberwinkler, P. Kruchten, M. Frotscher, E. Ziegler, A. Neugebauer, U. Bhoga, E. Bey, U. Müller-Vieira, J. Messinger, H. Thole, R.W. Hartmann, *J. Med. Chem.* 51 (2008) 4685–4698.
- [16] E. Bey, S. Marchais-Oberwinkler, P. Kruchten, M. Frotscher, R. Werth, A. Oster, O. Algül, A. Neugebauer, R.W. Hartmann, *Bioorg. Med. Chem.* 16 (2008) 6423–6435.
- [17] E. Bey, S. Marchais-Oberwinkler, M. Negri, P. Kruchten, A. Oster, T. Klein, A. Spadaro, R. Werth, M. Frotscher, B. Birk, R.W. Hartmann, *J. Med. Chem.* 52 (2009) 6724–6743.
- [18] S. Marchais-Oberwinkler, C. Henn, G. Möller, T. Klein, M. Negri, A. Oster, A. Spadaro, R. Werth, M. Wetzel, K. Xu, M. Frotscher, R.W. Hartmann, J. Adamski, *J. Steroid. Biochem. Mol. Biol.* 125 (2011) 66–82.
- [19] Y. Dong, Q.Q. Qiu, J. Debeer, W.F. Lathrop, D.R. Bertolini, P.P. Tamburini, *J. Bone Miner. Res.* 13 (1998) 1539–1546.
- [20] M. Feix, L. Wolf, H.U. Schweikert, *Mol. Cell. Endocrinol.* 171 (2001) 163–164.
- [21] L.J. Eyre, R. Bland, I.J. Bujalska, M.C. Sheppard, P.M. Stewart, M. Hewison, *J. Bone Miner. Res.* 13 (1998) 996–1004.
- [22] M. Wetzel, S. Marchais-Oberwinkler, R.W. Hartmann, *Bioorg. Med. Chem.* 19 (2011) 807–815.
- [23] M. Wetzel, S. Marchais-Oberwinkler, E. Perspicace, G. Möller, J. Adamski, R.W. Hartmann, *J. Med. Chem.* 54 (2011) 7547–7557.
- [24] K. Xu, Y.A. Al-Soud, M. Wetzel, R.W. Hartmann, S. Marchais-Oberwinkler, *Eur. J. Med. Chem.* 46 (2011) 5978–5990.
- [25] S. Marchais-Oberwinkler, K. Xu, M. Wetzel, E. Perspicace, M. Negri, A. Meyer, A. Odermatt, G. Möller, J. Adamski, R.W. Hartmann, *J. Med. Chem.* 56 (2013) 167–181.
- [26] E. Perspicace, A. Giorgio, A. Carotti, S. Marchais-Oberwinkler, R.W. Hartmann, *Eur. J. Med. Chem.* 69 (2013) 201–205.
- [27] K. Xu, M. Wetzel, R.W. Hartmann, S. Marchais-Oberwinkler, *Lett. Drug Des. Discov.* 8 (2011) 406–421.
- [28] Y.A. Al-Soud, S. Marchais-Oberwinkler, M. Frotscher, R.W. Hartmann, *Arch. Pharm.* 345 (2012) 610–621.
- [29] M. Wetzel, E.M. Gargano, S. Hinsberger, S. Marchais-Oberwinkler, R.W. Hartmann, *Eur. J. Med. Chem.* 47 (2012) 1–17.
- [30] E. Perspicace, S. Marchais-Oberwinkler, R.W. Hartmann, *Molecules* 18 (2013) 4487–4509.
- [31] A.E.F. Nassar, A.M. Kamel, C. Clarimont, *Drug Discov. Today* 9 (2004) 1020–1028.
- [32] E.H. Kerns, L. Di, *Drug-like Properties: Concepts, Structure Design and Methods from ADME to Toxicity Optimization*, first ed., Elsevier Inc., United States of America, 2008, pp. 329–330.
- [33] T.N. Thompson, *Med. Res. Rev.* 21 (2001) 412–449.
- [34] P. Valadon, P.M. Dansette, J.P. Girault, C. Amar, D. Mansuy, *Chem. Res. Toxicol.* 9 (1996) 1403–1413.
- [35] J.St. Jean, Jr. David, C. Fotsch, *J. Med. Chem.* 55 (2012) 6002–6020.
- [36] H. Fiesselmann, F. Thoma, *Chem. Ber.* 89 (1956) 1907–1912.
- [37] K.M. Sam, S. Auger, V. Luu-The, D. Poirier, *J. Med. Chem.* 38 (1995) 4518–4528.
- [38] W. Qiu, R.L. Campbell, A. Gangloff, P. Dupuis, R.P. Boivin, M.R. Tremblay, D. Poirier, S.-X. Lin, *FASEB J.* 16 (2002) 1829–1831.
- [39] P. Kruchten, R. Werth, S. Marchais-Oberwinkler, M. Frotscher, R.W. Hartmann, *Mol. Cell. Endocrinol.* 301 (2009) 154–157.
- [40] E. Bey, S. Marchais-Oberwinkler, R. Werth, M. Negri, Y.A. Al-Soud, P. Kruchten, A. Oster, M. Frotscher, B. Birk, R.W. Hartmann, *J. Med. Chem.* 51 (2008) 6725–6739.
- [41] C.A. Lipinski, F. Lombardo, B.W. Dominy, P.J. Feeney, *Adv. Drug Deliv. Rev.* 23 (1997) 3–25.
- [42] E. Perspicace, L. Cozzoli, E.M. Gargano, N. Hanke, A. Carotti, R.W. Hartmann, *Eur. J. Med. Chem.* 83 (2014) 317–337.
- [43] G. Drehesen, J. Engel, *Sulfur Rep.* 3 (1983) 171–207.
- [44] EDSP, Protocol for the In Vitro Estrogen Receptor Saturation Binding and Competitive Binding Assays Using Rat Uterine Cytosol, 2009. Available via EPA: http://www.epa.gov/endo/pubs/assayvalidation/appendix1_er_ruc.pdf.
- [45] L. Di, E.H. Kerns, Y. Hong, T.A. Kleintop, O.J. McConnell, D.M. Hury, *J. Biomol. Screen* 8 (2003) 453–462.
- [46] J. Moreno-Farre, P. Workman, F. Raynaud, *Aust.-Asian J. Cancer* 6 (2007) 55–69.
- [47] J.P.M. Hui, J.S. Grossert, M.J. Cutler, J.E. Melanson, *Rapid. Commun. Mass Spectrom.* 26 (2011) 345–354.
- [48] T. Thiemann, D.J. Walton, A. Olivera Brett, J. Iniesta, F. Marken, Y.Q. Li, *Arxiv* 9 (2009) 96–113.
- [49] C.S. Leung, S.S.F. Leung, J. Tirado-Rives, W.L. Jorgensen, *J. Med. Chem.* 55 (2012) 4489–4500.
- [50] D.W. Zhu, X. Lee, R. Breton, D. Ghosh, W. Pangborn, W.L. Daux, S.X. Lin, *J. Mol. Biol.* 234 (1993) 242–244.
- [51] S.X. Lin, F. Yang, J.Z. Jin, R. Breton, D.W. Zhu, V. Luu-The, F. Labrie, *J. Biol. Chem.* 274 (1992) 28762–28770.
- [52] K.M. Sam, R.P. Boivin, M.R. Tremblay, S. Auger, D. Poirier, *Drug Des. Discov.* 15 (1998) 157–180.